frontiers in Marine Science

ORIGINAL RESEARCH
published: 14 October 2021
doi: 10.3389/fmars.2021.752945

Extreme Runoff of Chemical Species of Nitrogen and Phosphorus Threatens a Florida Barrier Island Lagoon

John H. Trefry and Austin L. Fox*

Department of Ocean Engineering and Marine Science, Florida Institute of Technology, Melbourne, FL, United States

Extreme runoff of stormwater to poorly flushed barrier island lagoons often adds excess nitrogen (N) and phosphorus (P) that can promote subsequent, sometimes intense, harmful algal blooms (HABs). Successful management of such estuaries requires special appreciation of when and how to control concentrations and fluxes of chemical species of N and P during high flow. Toward that end, monthly surveys and episodic rain-event sampling were carried out from December 2015 to March 2018 for two contrasting tributaries of the Indian River Lagoon (IRL), a barrier island lagoon in Florida. One tributary, South Prong Saint Sebastian River, flows through predominantly agricultural, forested and open land, whereas the second tributary, Crane Creek, traverses mainly residential-commercial land. Concentrations of some N and P species in these tributaries increased with increased flow and could be described with statistically significant equations for concentration versus flow rate, thereby supporting flow-rate-dependent flux determinations. Drainage basin yields (fluxes per square km) varied with land cover/use. Calculated annual yields of dissolved organic N (DON) and dissolved inorganic P (DIP) averaged ∼70% greater for South Prong Saint Sebastian River from high flow through thicker, more organic- and P-rich soils. In contrast, yields of nitrate + nitrite were 100% higher for Crane Creek from widespread application of N-fertilizer to thin layers of turfgrass overlying sand, plus runoff of N-rich reclaimed water. Two major weather events highlighted our study and foreshadow impacts from climate change. Seven months of drought from November 2016 to May 2017 were followed in September-October 2017 by excess rain, runoff and flooding from Hurricane Irma. Consequently, >50% of freshwater fluxes and ∼60% of N and P fluxes from South Prong Saint Sebastian River, Crane Creek and other IRL tributaries occurred during 2 months in 2017. Lagoon-wide inputs provided enough bioavailable N and P to help support a nanoeukaryotic bloom for >5 months, with chlorophyll *a* values >50 $\mu g\ L^{-1}$. The bloom was co-dominated by the brown tide alga, *Aureoumbra lagunensis*, and an unidentified nanoeukaryotic green alga. Decreased salinity, low concentrations of dissolved inorganic N and P, and decreasing dissolved organic P (DOP), combined with biological factors, diminished the IRL bloom by mid-2018.

Keywords: Indian River Lagoon, nitrogen, phosphorus, dissolved organic nitrogen, dissolved inorganic nitrogen, *Aureoumbra lagunensis*

OPEN ACCESS

Edited by:
Edward J. Phlips,
University of Florida, United States

Reviewed by:
João Pedro Coelho,
University of Aveiro, Portugal
Lauren M. Hall,
St. Johns River Water Management District, United States

****Correspondence:***
John H. Trefry
jtrefry@fit.edu

Specialty section:
This article was submitted to Marine Pollution, a section of the journal Frontiers in Marine Science

Received: *04 August 2021*
Accepted: *17 September 2021*
Published: *14 October 2021*

Citation:
Trefry JH and Fox AL (2021) Extreme Runoff of Chemical Species of Nitrogen and Phosphorus Threatens a Florida Barrier Island Lagoon. Front. Mar. Sci. 8:752945. doi: 10.3389/fmars.2021.752945

INTRODUCTION

Nutrient inputs from human activities have caused a worldwide crisis of eutrophication in estuaries and the coastal ocean (Diaz and Rosenberg, 2008). Ongoing climate change further accelerates eutrophication when increased evaporation and precipitation, spurred by solar heating and more powerful tropical storms, intensify runoff and seaward transport of nutrients (Trenberth and Asrar, 2014; Bhatia et al., 2019). Coincidently, concentrations of some chemical species of nitrogen (N) and phosphorus (P) increase during high flow rates in creeks and rivers (Dierberg, 1991; Chen et al., 2015). For example, higher concentrations of phosphate and dissolved organic matter have been reported for many tributaries during storms because of enhanced desorption and remineralization of organic matter and nutrients as water flows through upper, organic-rich soil horizons (Chen et al., 2015; Jeanneau et al., 2015). Poorly flushed, barrier island lagoons can trap runoff from large storms for weeks to months, subsequently increasing the potential for harmful algal blooms (HABs; Steward et al., 2006; Cira and Wetz, 2019). Therefore, management strategies that improve upstream water retention and lagoon water quality must consider when and how concentrations and fluxes of N and P species respond to increased flow rates.

Human-induced changes in land use are well known to enhance nutrient transport to estuaries (Bussi et al., 2017). Expanded residential development increases impervious surface area that can lead to exponential increases in nitrate concentrations from fertilizer runoff or septic system sources (Cunningham et al., 2009). Increased agricultural land use has been linked to higher concentrations and fluxes of phosphate, ammonium and nitrate + nitrite (Chen et al., 2013; Wang et al., 2015). Loading of suspended solids bearing N and P often increases during high water flow, especially after land clearing (Jordan et al., 2018). The quantity and quality of water carried by tributaries as a function of land use is clearly an important and complex component of predicting the health of estuaries (Pellerin et al., 2006; Osburn et al., 2016).

Annual nutrient exports to estuaries and the coastal ocean have been estimated at 43 Tg of total N (TN) and 9 Tg of total P (TP; Seitzinger et al., 2010; Oelsner and Stets, 2019). This TN was 44% dissolved inorganic N (ammonium and nitrate + nitrite), 31% particulate N (PN) and 25% dissolved organic N (DON) whereas TP included 77% particulate P, 16% dissolved inorganic P (DIP) and 7% dissolved organic P (DOP; Seitzinger et al., 2010). About 40% of river borne total dissolved N (TDN) and 50% of total dissolved P (TDP) were estimated to be of anthropogenic origin (Berner and Berner, 2012). DON comprises sub-groups including amino acids and humic substances as well as specific molecules such as urea, a common component of fertilizer (Watanabe et al., 2014; Feng et al., 2016; Ivey et al., 2020). PN includes adsorbed inorganic N (e.g., ammonium) as well as living and dead organic matter. DOP includes adenosine triphosphate (ATP), phospholipids and phosphonic acids (Van Mooy et al., 2015; Diaz et al., 2018). Particulate P is composed of inorganic P (P minerals containing Ca or Fe as well as P adsorbed to particles) and organic forms of adsorbed and intracellular P (Labry et al., 2013).

Seasonal fluxes of anthropogenic nutrients from tributaries to estuaries can be strongly influenced by severe storms (Paerl et al., 2001; Wetz and Yoskowitz, 2013; Phlips et al., 2020). Paerl et al. (2001) observed large increases in concentrations of dissolved inorganic N and dissolved organic carbon (DOC), along with delivery of at least half the annual N load, to Pamlico Sound during passage of three sequential hurricanes in September-October 1999. A wide variety of storm-related impacts on water quality, seagrass beds, nutrient exports and phytoplankton productivity were described in a synthesis by Wetz and Yoskowitz (2013). They showed that extreme climatic events alter delivery and processing of nutrients and physicochemical properties of estuaries.

Steady advances in determining biochemical uptake rates for a variety of inorganic and organic forms of N and P by plankton and bacteria have occurred during the past several decades (Björkman and Karl, 1994; Kang et al., 2015; Diaz et al., 2018). Laboratory incubation experiments by Wiegner et al. (2006) showed that ∼23% of river-borne DON can be biologically available, relative to only ∼4% of dissolved organic C. Laboratory studies also indicated that the brown tide alga, *Aureoumbra lagunensis*, took up ammonium and urea very rapidly, but was unable to use nitrate (Deyoe and Suttle, 1994). A study of P uptake by cyanobacteria confirmed uptake of ATP; however, uptake of phosphate was at a three to fourfold faster rate (Michelou et al., 2011). These advances all show the importance of knowing which N and P species make up TN and TP in tributaries and estuaries.

Our study focused on the Indian River Lagoon (IRL), a barrier island lagoon along the east central coast of Florida, United States (**Figure 1**). The IRL is presently experiencing an environmental crisis in the form of poor water quality, intense algal blooms, a 50% decline in seagrass area, fish kills and manatee mortality (Kang et al., 2015; Lapointe et al., 2020; Phlips et al., 2020). These impacts are now transforming the lagoon from a macrophyte-based system to an algae-based system (Sigua and Tweedale, 2003; Phlips et al., 2015, 2020). Included among HABs in the IRL were blooms of the brown tide alga, *Aureoumbra lagunensis*, in 2012-2013, 2015-2016, and 2017-2018 (Kang et al., 2015; Phlips et al., 2015, 2021; Judice et al., 2020). Loading of N and P is certainly a primary driver of HABs and the present condition of the IRL (Sigua and Tweedale, 2003; Lapointe et al., 2020).

The overall goal of this study was to improve our understanding of concentrations and runoff fluxes of N and P species transported to the IRL by tributaries and to identify connections to HABs in the lagoon. The term runoff is used here as the combined volume of surface runoff plus baseflow (i.e., groundwater). Our specific objectives for the IRL included the following: (1) determine mathematical relationships for concentrations of N and P species in two contrasting tributaries versus flow rate, (2) calculate fluxes of N and P species from the two tributaries, (3) identify drainage basin controls on nutrient fluxes and (4) relate tributary inputs of N and P species to subsequent phytoplankton blooms in the IRL, particularly a bloom involving *Aureoumbra lagunensis* following Hurricane

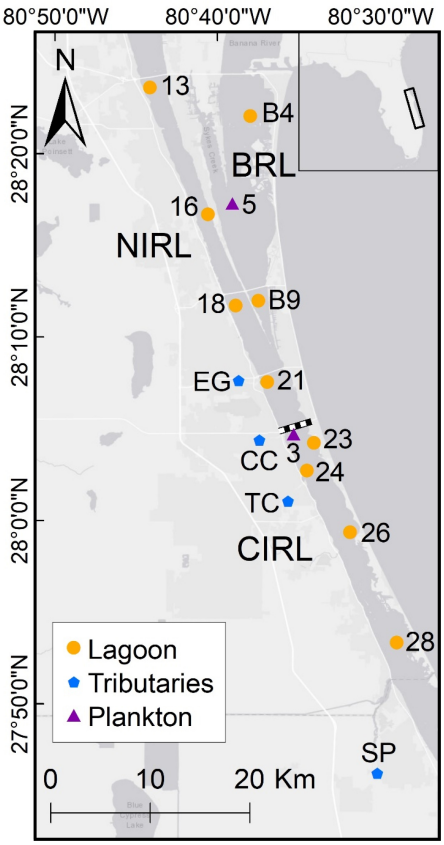

FIGURE 1 | Map of Indian River Lagoon (IRL) showing tributaries South Prong Saint Sebastian River (SP), Crane Creek (CC), Turkey Creek (TC), and Eau Gallie River (EG). Boundary between North IRL (NIRL) and Central IRL (CIRL) shown with dashed line north of CC. IRL stations 13, 16, 18, 21, 23, 24, 26, and 28 plus Banana River Lagoon (BRL) stations B4 and B9 were sampled by St. Johns River Water Management District [SJRWMD] (2020b). Phytoplankton were sampled by Phlips et al. (2021). Sebastian Inlet to the Atlantic Ocean is ∼5 km east of the mouth of SP. Inset map shows IRL and BRL along central east coast of Florida. Station coordinates in **Supplementary Table 1**.

Irma in 2017. The primary application of this effort was to help improve management activities that control freshwater and nutrient runoff, HABs and water quality in the IRL.

MATERIALS AND METHODS

Study Area

Indian River Lagoon spans 250 km along the central east coast of Florida with five inlets to the Atlantic Ocean. The barrier island is continuous, without any inlets, along ∼140 km of the Central IRL, North IRL and Banana River Lagoon (BRL) from Sebastian Inlet north through our study area to Ponce Inlet. In this study, we investigated four tributaries, one in North IRL (Eau Gallie River) and three in Central IRL (Crane Creek, Turkey Creek and South Prong Saint Sebastian River) (**Figure 1**). Three of these four tributaries, excluding Eau Gallie River, have no causeway between them and Sebastian Inlet. The fourth tributary, Eau Gallie River, is ∼5 km north of Crane Creek (**Figure 1**). Surface water flow into the IRL and BRL north of Eau Gallie River is primarily *via* smaller creeks, outfalls, ditches and diffuse runoff. Detailed investigations for 2016 and 2017 were carried out for all four tributaries. Two tributaries, South Prong Saint Sebastian River and Crane Creek, with contrasting land use and land cover, are discussed in detail here. South Prong Saint Sebastian River (hereafter referred to in the text as South Prong) has the largest drainage basin in the overall Saint Sebastian River system and is a representative subbasin with respect to land use and soil type (Gao and Rhew, 2013). South Prong and Crane Creek have received special attention by the State of Florida for total maximum daily loads (TMDLs) of nutrients (Gao and Rhew, 2013; Harper and Baker, 2013). Data for all four tributaries were compiled in a report by Trefry et al. (2019); references to Turkey Creek and Eau Gallie River are made when applicable to the Discussion.

South Prong and Crane Creek (**Figure 1**) are separated by ∼36 km and have similar geomorphology and average land elevations ∼9 m. The South Prong drainage basin in Indian River County occupies 146 km^2 with median annual daily flow of 2.9 ± 0.8 m^3 s^{-1} relative to 32.6 km^2 and 0.59 ± 0.20 m^3 s^{-1} for Crane Creek in Brevard County (Bergman et al., 2002; Gao and Rhew, 2013; United States Geological Survey [USGS], 2020b,d). The Turkey Creek drainage basin spans 254 km^2 with median annual daily flow of 4.1 m^3 s^{-1} relative to 24 km^2 and 0.34 m^3 s^{-1} for Eau Gallie River (United States Geological Survey [USGS], 2020a,c). Despite their small sizes, the four IRL tributaries have an average annual water runoff [flow/basin area = (km^3 y^{-1})/km^2); m y^{-1}] of 0.55 m y^{-1}, double the average for all continents except South America with 0.68 m y^{-1} (Berner and Berner, 2012).

Land use in the South Prong drainage basin is 17% residential-commercial, 33% agricultural, and 50% undeveloped wetlands, forested and open land whereas Crane Creek is 67% residential-commercial, <2% agricultural and 31% undeveloped wetlands, forested and open land (Gao and Rhew, 2013). Land use in Turkey Creek and Eau Gallie River is >59 and >71% urban, respectively (Trefry et al., 2019). Nutrients transported from South Prong to Central IRL have an increased likelihood of being exported to the coastal Atlantic Ocean because of proximity of South Prong to Sebastian Inlet (**Figure 1**). The wet season in the IRL is presently defined as June 1-October 31 and the dry season as November 1-May 31. A fertilizer ban from June 1 to September 30 has been in effect since 2014 for both drainage basins; P-containing fertilizers are not permitted for turfgrass at any time in both areas. Large inputs of freshwater and nutrients from other tributaries and outfalls in the North IRL and BRL have monthslong residence times where they can promote HABs (Steward et al., 2005).

Sampling

Tributary surveys were carried out monthly from December 2015 to March 2018 and episodically during 1- to 7-day rain events (i.e., when rainfall was predicted to be >2.5 cm). South Prong and Crane Creek were sampled from bridges near USGS flow gauges (**Figure 1**). During each survey, vertical profiles

for conductivity, temperature, pH and dissolved oxygen were obtained prior to sampling using a YSI 6600 V2. The sonde was calibrated at the beginning of each day following manufacturer's specifications and successfully intercalibrated with a YSI ProDSS when it replaced the 6600 V2 in 2017. Sampling locations were upstream of their respective salt wedges; the water was typically <2 m deep and well mixed. Water samples were collected in acid-washed, low-density polyethylene bottles. The open bottles were placed in a weighted plastic holder and lowered from a bridge to the surface of the water and then quickly (1–2 s) lowered to a water depth of ∼0.5 m using a marked rope. Samples were placed in coolers until returned to the Marine & Environmental Chemistry Laboratories at Florida Institute of Technology (FIT) where filtration was carried out in a laminar flow hood within 2–3 h of collection. Supporting data for stations in the IRL (n = 8) and BRL (n = 2; **Figure 1**) were obtained from the St. Johns River Water Management District (St. Johns River Water Management District [SJRWMD], 2020a,b). Data and methods for biomass calculations of phytoplankton are from Phlips et al. (2021). These data for water chemistry and phytoplankton biomass were used to discuss the consequences of stormwater runoff to the IRL after Hurricane Irma in September 2017. All station coordinates are listed in **Supplementary Table 1**.

Laboratory Analysis

Water for analysis of most dissolved and particulate chemicals was vacuum filtered through polycarbonate filters (Poretics, 47-mm diameter, 0.4-μm pore size) in a Class-100 laminar-flow hood in an FIT clean room with controlled temperature and relative humidity. Prior to the field effort, filters were acid washed in 3N HCl, rinsed three times with deionized water, dried and then weighed to the nearest μg. Each filter was weighed twice in random order, with a minimum of 5% of the filters being weighed in triplicate as described by Trefry and Trocine (1991). Samples for particulate organic carbon (POC) were filtered in a Class-100 laminar flow hood through pre-combusted (450°C) Gelman Type A/E glass fiber filters mounted on HCl-washed filtration glassware. All particle-bearing filters were sealed in separate, acid-washed petri dishes, labeled, double-bagged in plastic and stored dried and re-weighed to a constant weight.

Concentrations of ammonium, nitrate + nitrite, TDN, DIP, and TDP in the filtrate were determined using a SEAL AA3 HR Continuous Segmented Flow AutoAnalyzer following manufacturer's method G-218-98. For TDN analysis, organic and inorganic N compounds were converted to nitrate using UV irradiation and persulfate digestion. Nitrate was then reduced to nitrite using a cadmium column; analysis followed by UV-visible spectrometry. For TDP analysis, UV and persulfate digestion were used to free organically bound P for analysis by UV-visible spectrometry. We recognize that DIP is measured as soluble reactive phosphorus; we use DIP as a common term in marine sciences. The National Institute of Standards and Technology (NIST) traceable Dionex 5-Anion Standard was analyzed as a reference standard with each batch of samples to ensure accuracy; results were within established 95% confidence limits. Values for analytical precision as relative standard deviation (RSD) were as follows: ammonium (3%), nitrate + nitrite (6%), TDN (2%), DIP (3%) and TDP (3%). Procedural blanks were processed with each batch of samples. Concentrations of DON and DOP were calculated by subtracting the inorganic forms of each element from TN and TP, respectively. Precision was 4% for DON and 16% for DOP. Precision for DOP was weak when DIP was the dominant component of TDP. Detection limits (μM) were as follows: ammonium (0.5), nitrate + nitrite (0.1), TDN and DON (0.04), DIP (0.04), TDP and DOP (0.04).

Analysis for DOC was carried out using a Shimadzu TOC-5050A instrument with non-dispersive infrared detection. Concentrations were calculated by subtracting inorganic carbon from total carbon. Accuracy was determined using an NIST-traceable standard solution of potassium hydrogen phthalate (83.3 μM) from Inorganic Ventures; results were within 95% confidence limits. Precision averaged 1.9% (RSD) and the detection limit was 15 μ M.

Suspended particles captured on polycarbonate filters, as well as separate milligram quantities of standard reference material (SRM) #2704, a river sediment issued by the NIST, were digested in stoppered, 15-mL Teflon test tubes using Ultrex II HNO_3 and HF as described by Trefry and Trocine (1991). Concentrations of Al and Fe were determined by flame atomic absorption spectrometry using a Perkin-Elmer 4000 instrument and concentrations of P were determined by inductively coupled plasma mass spectrometry using a Varian 820 instrument. Concentrations of the three elements were within the 95% confidence intervals for the SRM. Analytical precision ranged from 1 to 5% as a function of sample mass and elemental concentrations. Detection limits (% of TSS) were as follows: Al (0.2), Fe (0.03), and P (0.01).

Concentrations of POC and PN were determined by first treating particles on the glass-fiber filter with 10% (v/v) hydrochloric acid to remove any inorganic carbon, then dried. Organic N was not lost during this process based on our laboratory testing. Filters with 200–800 mg of pre-treated suspended sediment were weighed into ceramic boats and combusted with pure oxygen at 950°C using a LECO TruMac C/N/S system. Quantification of the resultant CO_2 and N_2 gases was *via* infrared and thermal conductivity detectors, respectively. Concentrations of C and N in sediment SRM #2704 and LECO reference sample 502–309 were within 95% confidence intervals for certified values. Analytical precision was 1.5% for POC and 2% for PN. Detection limits (% of TSS) were as follows: POC (0.2) and PN (0.3).

Calculations and Data Interpretation

Data and graphical analyses were carried out using Systat 12 and SigmaPlot 10 (Systat Software, Inc.), Excel 2016 (Microsoft) and ArcGIS (Version 10.2.2.3552, Esri, Redlands, CA, United States). An alpha value to define statistical significance was set at 0.05 for statistical tests and regressions. Least squares linear regressions were calculated to determine relationships between individual pairs of parameters (e.g., DON versus flow rate). Equations, 95% prediction intervals, correlation coefficients (r) and p values were determined for each relationship. General descriptors used for r values were as follows: >0.4-0.6 (moderate), >0.6-0.8 (moderately strong), >0.8-0.9 (strong) and >0.9 (very

strong). Comparisons of two independent groups of data were carried out using two-tailed *t*-tests assuming equal variance. Independent groups of data with *p*-values >0.05 were considered not significantly different from one another. Statistics for the 2016-2017 data were calculated using results for monthly samples to keep sampling days the same for both tributaries. Sampling for rain events took place on a variety of different days for each tributary, with some overlap.

Annual mass fluxes of nutrients and other chemicals from each tributary during 2016 and 2017 were calculated using two approaches. When a significant correlation ($p < 0.05$) was obtained for concentrations of a chemical for monthly and storm samples versus log flow rate (Q), the pertinent equation was used to calculate the concentration for each day using daily flow rate data from the United States Geological Survey [USGS], 2020b,d. Log flow rate was used in Eq. 1 because non-linear changes in concentration versus flow rate were observed and log flow rate has been successfully used in linear regressions for flow rate versus concentrations of dissolved organic C (Smith and Kaushal, 2015) and nitrate (Duncan et al., 2017). No differences in calculated concentrations were found by using natural (ln) versus base 10 logarithms (log) for our flow rates. The mass flux in t y^{-1} (J) was determined from the sum of daily transport (Eq. 1).

$$J = \sum_{i=1}^{365} [(a * \log Q\ (i) + b) * Q\ (i)] \quad (1)$$

where [a * log Q + b] is the general equation for concentrations of a chemical versus flow rate and Q is the average daily flow rate from the United States Geological Survey [USGS], 2020b,d. When a regression equation for a chemical versus flow rate was not significant, and the data grouped around the median (M) for the chemical, Eq. 2 was used with median concentrations and daily flow rates.

$$J = \sum_{i=1}^{365} [M * Q\ (i)] \quad (2)$$

Equations for chemicals versus flow rates are listed in **Supplementary Table 2**. We used water flow at the time of sampling on graphs and in calculating fluxes for consistency. A few outlying data points were omitted, as noted, in calculating chemical versus flow rate equations because they were outside the mean by two standard deviations and/or had a clear explanation for the anomaly.

RESULTS

Rainfall and Runoff

Two major weather events highlighted our 2016-2017 study period. First, an extended drought spanned November 2016 through May 2017 (**Figures 2A-D**). Second, this drought was followed by excess rainfall, runoff and flooding that began with passage of Hurricane Irma in early September 2017. Rainfall continued through October and flooding did not abate until late November 2017 (**Figures 2C,D**). The tributaries, outfalls and IRL all experienced these weather events.

Annual rainfall during 2016 in the South Prong and Crane Creek drainage basins was 162 and 166 cm, respectively (**Figures 2A,B**), relative to 30-year averages of 142 cm for South Prong and 122 cm for Crane Creek (National Oceanic and Atmospheric Administration [NOAA], 2020). During 2017, rainfall was 7 and 30% higher, respectively, for Crane Creek and South Prong than in 2016 (**Figures 2C,D**). Greater rainfall in South Prong during 2017, relative to Crane Creek, occurred because its larger drainage basin extended farther inland and closer to the storm track of Hurricane Irma (Cangialosi et al., 2018). Rainfall during both years in both drainage basins was above the 80th percentile for the past 20 years (National Oceanic and Atmospheric Administration [NOAA], 2020). In 2017, only ∼13% of rainfall in both basins occurred during 5 months of drought (January through May) relative to 40 and 53% in South Prong and Crane Creek, respectively, during September and October (**Figures 2C,D**).

Annual runoff in South Prong during 2017 was 50% higher than in 2016 due to greater rainfall and flooding associated with Hurricane Irma (**Figures 2A,C**). In contrast, annual flow from Crane Creek in 2017 was only 11% higher than in 2016 because rainfall was only ∼6% greater and high flow was during September and October, relative to June-December for South Prong (**Figures 2A-D**).

Dissolved Chemicals

Total dissolved solids (TDS) peaked at ∼1,400 mg L^{-1} in South Prong and ∼900 mg L^{-1} in Crane Creek from infiltration of groundwater during the November 2016-May 2017 period of drought (**Figures 3A,B**). Groundwater in artesian wells and the upper Floridan Aquifer in the study area have TDS values of 1,000-4,000 mg L^{-1} (Kroening, 2004). Lowest TDS of 300-500 mg L^{-1} in both tributaries occurred during high flow, including Hurricanes Matthew in October 2016 and Irma in September 2017 (**Figures 3A,B**). During storm events, TDS in both tributaries often decreased by half within the first 12 h *via* dilution with rainwater (**Supplementary Figure 1**). A return to median values typically occurred within ∼1 day after rainfall stopped at Crane Creek, but >4-day in the larger and less well drained South Prong basin (**Supplementary Figure 1**). Statistically significant equations with correlation coefficients equal to −0.86 (South Prong) and −0.90 (Crane Creek) were calculated for TDS versus flow rate (**Figures 3C,D**). Correlations for dissolved chemical species versus TDS, when significant, were used to help assess the relative importance of surface runoff versus baseflow (groundwater) to nutrient concentrations and fluxes. Higher TDS and a positive correlation with dissolved chemical species suggested a substantial contribution from groundwater during low flow (O'Connor, 1976).

Both IRL tributaries had median concentrations of DON of 30-35 μM (**Table 1**) and ranges of <20 μM to >60 μM (**Figures 3E,F**). DON was the dominant form of TN in South Prong (57%) and Crane Creek (48%), a common, but not universal feature of rivers (Pellerin et al., 2006; Wiegner et al., 2006; Lorite-Herrera et al., 2009). Concentrations of DON in South Prong, but not Crane Creek, showed a strong positive correlation versus log flow rate (**Figures 3G,H**). Concentrations

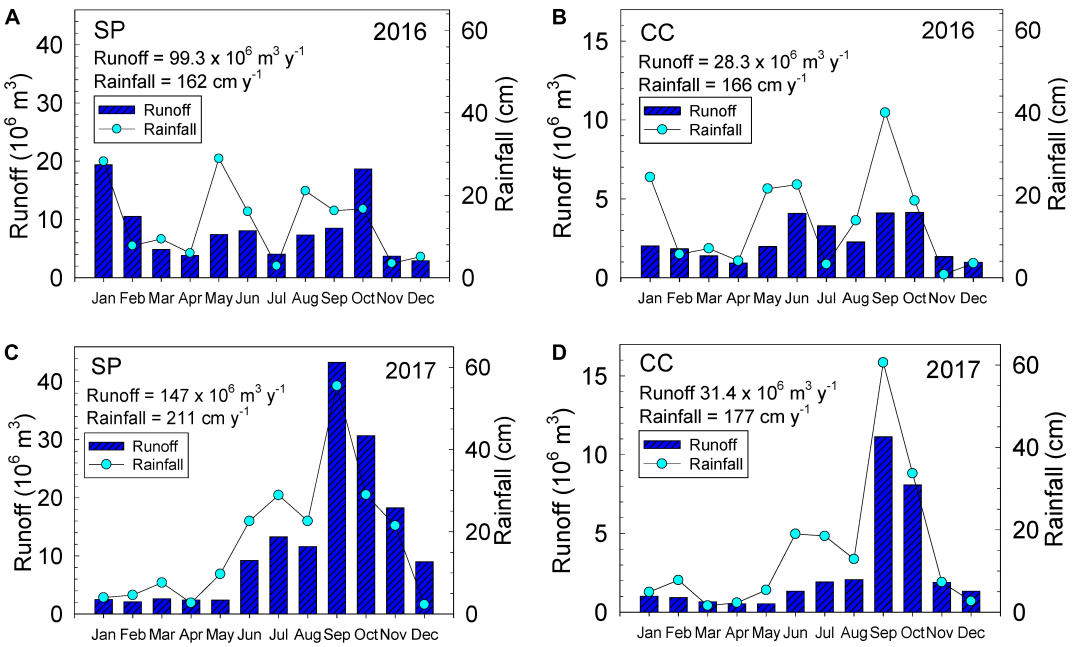

FIGURE 2 | Monthly rainfall and runoff during 2016 and 2017 for **(A,C)** South Prong Saint Sebastian River (SP) and **(B,D)** Crane Creek (CC). Totals for each year shown on upper left of graphs. Rainfall data from National Oceanic and Atmospheric Administration [NOAA] (2020) and runoff from United States Geological Survey [USGS] (2020b,d).

of DON in South Prong, but not Crane Creek, were well above the median during rain events (**Supplementary Figure 1**). A strong negative correlation for DON versus TDS was obtained for St. Sebastian ($r = -0.88$, $p < 0.001$), but not for Crane Creek (**Supplementary Figure 1**).

Mean values for nitrate + nitrite and ammonium were about twofold higher in Crane Creek than in South Prong (**Table 1**). Nitrate + nitrite accounted for 29% of TN in Crane Creek, but only 13% in South Prong. The average % of TN that was ammonium was 6 ± 2% for South Prong and 8 ± 5% for Crane Creek. Highest concentrations for these N species in both tributaries were generally found at median flow; lowest concentrations were commonly observed during high flow (**Figures 4A–D**). Concentrations of nitrate + nitrite (**Figure 4C**) and ammonium did not correlate significantly with flow rate for South Prong, likely because of complex relationships with flow and other variables. For Crane Creek, a significant negative correlation was obtained for nitrate + nitrite versus log flow rate (**Figure 4D**), but not for ammonium versus log flow rate (**Supplementary Table 2**).

Total P and DIP showed parallel patterns versus flow rate in both tributaries with greater values during high flow (**Figures 4E,F**). Offsets between concentrations of TP and DIP shown on graphs were larger during high flow because of increases in particulate P concentrations (**Figures 4E,F**). DIP comprised 48% of TP in both tributaries. Concentrations of DIP increased above the median during rain events in both tributaries (**Supplementary Figure 1**). Following Hurricane Irma, concentrations of DIP were >30 μM in South Prong (**Figure 4E**). During drought conditions, mean DIP values of 1.3 μM in South Prong were threefold lower than the monthly average and >20 times lower than maximum values during rain events and hurricanes (**Figure 4E**). DIP values in both tributaries correlated positively with log flow rate; however, the slope for South Prong was ∼5 times greater than for Crane Creek (**Figures 4G,H**). DIP correlated significantly and negatively with TDS for South Prong, but not for Crane Creek.

Median concentrations of DOC for both South Prong and Crane Creek averaged ∼1,000 μM (**Table 1**) with a range of 300-2,600 μM; higher values occurred during increased flow (**Supplementary Figure 2**). An equation for DOC versus log flow rate for South Prong had a stronger positive correlation and a fourfold greater slope than the equation for Crane Creek (**Supplementary Figure 2**). A moderately strong negative correlation for DOC versus TDS ($r = -0.78$; $p < 0.001$) was obtained for South Prong, but not for Crane Creek.

Suspended Solids and Particulate Chemicals

Mean values for total suspended solids (TSS) in both tributaries during monthly surveys were <10 mg L^{-1} (**Table 1**). Such low TSS values were found in <5% of rivers globally; moreover, 40% of world rivers have mean TSS >500 mg L^{-1} (Meybeck et al., 2003). South Prong had significantly higher TSS than Crane Creek (**Table 1**). TSS generally increased with higher water flow in both tributaries (**Supplementary Figure 3**). Common to many rivers, higher TSS values were sometimes found during the onset of very high flow (i.e., "first flush" effect) with decreases over the duration of the rain event (**Supplementary Figure 3**). TSS

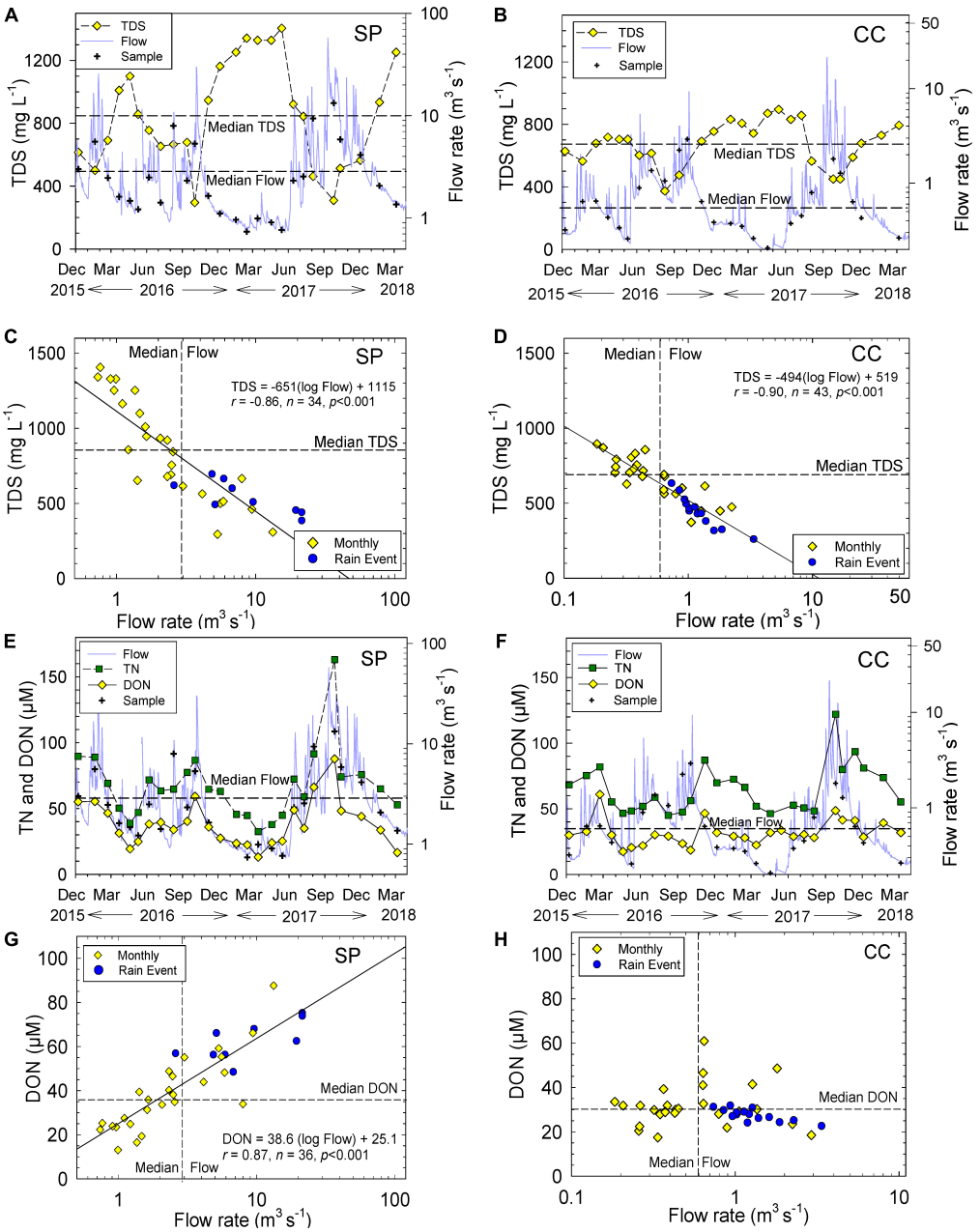

FIGURE 3 | Total dissolved solids (TDS) and flow rate for monthly samples at **(A)** South Prong Saint Sebastian River (SP) and **(B)** Crane Creek (CC). TDS versus flow rate for **(C)** SP and **(D)** CC. Total nitrogen (TN), dissolved organic nitrogen (DON) and flow rate for **(E)** SP and **(F)** CC. DON versus flow rate for **(G)** SP and **(H)** CC. Equations and lines on **(C,D,G)** from linear regression, with correlation coefficient (*r*), number of samples (*n*) and *p* statistic. Median concentrations are for monthly samples.

correlated significantly with log flow rate for both tributaries (**Supplementary Figure 3**).

Concentrations of POC (μM) in South Prong averaged ∼80% greater than in Crane Creek because of higher TSS in South Prong (**Table 1**). Despite overall low POC concentrations (μM) in both tributaries, the percentage of TSS that was POC averaged 15.5% (South Prong) and 17.9% (Crane Creek), much higher than a global mean of 1.7% (Kandasamy and Nath, 2016). PN values (μM) in South Prong averaged 52% higher relative to Crane Creek (**Table 1**) and ∼10-fold greater (% of TSS; **Table 1**) than a mean value of 0.3% for world rivers (Paolini, 1995). No significant difference was found for particulate P (μM) in South Prong versus Crane Creek (**Table 1**); however, South Prong and Crane Creek contained 2.3- and 3.7-fold higher amounts of particulate P (% of TSS, **Table 1**), respectively, than an average of 0.3% P for global rivers (Viers et al., 2009). PN accounted for 24 and 15% of

TABLE 1 | Means ± standard deviations (SD) and medians for concentrations of chemicals during monthly surveys, December 2015–March 2018.

Parameter	South Prong Saint Sebastian River (*n* = 26)		Crane Creek (*n* = 27)		*p* Value
	Mean ± SD	Median	Mean ± SD	Median	
Total Dissolved Solids (mg L^{-1})	860 ± 330	850	670 ± 140	690	0.0083
Total Suspended Solids (mg L^{-1})	9.8 ± 6.6	8.2	5.0 ± 5.0	3.1	0.0043
pH	7.63 ± 0.47	7.57	7.19 ± 0.45	7.19	0.0012*
Total N (μM)	66.7 ± 25.9	64.7	64.8 ± 18.5	57.5	0.76
Dissolved Organic N (μM)	38.3 ± 17.0	35.4	31.7 ± 9.6	30.0	0.086
Nitrate + Nitrite (μM)	8.0 ± 2.8	7.7	18.4 ± 7.6	17.3	<0.0001
Ammonium (μM)	3.8 ± 1.8	3.5	6.3 ± 6.7	3.2	0.072
Particulate N (μM)	16.6 ± 12.6	13.7	10.9 ± 8.7	8.7	0.06
Dissolved Inorganic N (μM)	11.9 ± 4.0	11.2	24.8 ± 11.3	21.8	<0.0001
Total Dissolved N (μM)	50.1 ± 17.8	48.3	56.5 ± 16.4	51.0	0.18
Total P (μM)	7.2 ± 4.6	4.6	4.2 ± 1.7	3.9	0.0026
Dissolved Inorganic P (μM)	4.0 ± 7.4	1.9	1.9 ± 0.4	1.8	0.15
Dissolved Organic P (μM)	1.0 ± 1.2	0.3	1.0 ± 1.0	1.6	1.00
Particulate P (μM)	2.2 ± 2.4	1.7	1.5 ± 0.90	1.2	0.16
Dissolved Organic Carbon (μM)	1130 ± 540	1100	875 ± 312	920	0.039
Particulate Organic Carbon (μM)	119 ± 72	100	66 ± 55	50	0.0040
Particulate Organic C (% of TSS)	15.5 ± 2.6	15.5	17.9 ± 4.2	18.6	0.016
Particulate N (% of TSS)	2.9 ± 1.5	2.6	3.7 ± 1.8	4.0	0.085
Particulate P (% of TSS)	0.69 ± 0.41	0.62	1.1 ± 0.3	1.2	<0.0001
Particulate Fe (% of TSS)	6.6 ± 1.4	6.7	10.7 ± 2.6	11.1	<0.0001
Particulate Al (% of TSS)	4.3 ± 1.4	4.3	2.8 ± 1.0	2.5	<0.0001

*p values from t-test >0.05 for mean values that are not statistically different. *p value calculated using concentrations and standard deviations for $[H^+]$ in molar units.*

TN in South Prong and Crane Creek, respectively, and particulate P accounted for 35% of TP in both tributaries. The high C, N, and P content of tributary particles showed that, despite low TSS, both tributaries carried nutrient-rich particles to the IRL.

The grand mean for aluminum (Al) in suspended particles from both tributaries (3.6 ± 1.4% of TSS, $n = 51$) was within 20% of the average for IRL sediments (Al = 4.4 ± 1.4%, $n = 23$; Trefry and Trocine, 2011). In contrast, average values for particulate iron (Fe % of TSS) were very high at 6.6% in South Prong and 10.7% in Crane Creek relative to 2.6 ± 1.3% in IRL sediments (Trefry and Trocine, 2011). Therefore, Fe/Al ratios for tributary particles were 3-5 times higher than a mean of 0.6 reported for IRL sediments (Trefry and Trocine, 2011).

Fluxes of Water Plus Dissolved and Particulate Chemicals

Monthly patterns for water flow to the IRL from both tributaries in 2016 were distinctly different than in 2017 (**Figure 2**). South Prong and Crane Creek transported only 10% of their annual water flow during the drought of January-May 2017, relative to 46% (South Prong) and 30% (Crane Creek) of annual flow from January-May 2016 (**Figure 2**). In 2017, >50% of the annual fluxes of water from both tributaries were exported to the IRL during September-October 2017, relative to <25% during the same period in 2016 (**Figure 2**). Similar trends during drought and extreme runoff in 2017 were observed throughout the Central IRL and North IRL (Trefry et al., 2019; United States Geological Survey [USGS], 2020a–d). The combination of 5 months of drought and 2 months of excess runoff and flooding in 2017 set up conditions for large-scale remobilization of nutrients from soils and large fluxes to the IRL.

Our calculated fluxes of TN and TP for 2016 from South Prong to the IRL were 106 t and 16.7 t, respectively (**Table 2**), similar to multi-year averages of 114 t for TN and 19 t for TP by Gao and Rhew (2013). Our fluxes for TN and TP in 2017 for South Prong were 60 and 80% greater, respectively, than in 2016 (**Table 2**). Gao and Rhew (2013) reported average fluxes from Crane Creek for TN (29 t) and TP (5.4 t) that were higher than our 2016 values and more like our 2017 values (**Table 2**). To better compare the tributary data, yields (fluxes divided by drainage basin area) were calculated. TN yields for both IRL tributaries matched within 6% for 2016; however, the TN yield in 2017 was 31% greater for South Prong than Crane Creek (**Table 2** and **Figures 5A,B**). Similar annual trends were observed for yields of TP for both tributaries (**Table 2** and **Figures 5C,D**).

In contrast with TN, yields for DON from South Prong were 32 and 115% greater in 2016 and 2017, respectively, than found for Crane Creek, even though water flow from Crane Creek was 28% greater in 2016 and only 5% less in 2017 (**Table 2** and **Figures 5E,F**). DON comprised an average of 46% of the TN yield for Crane Creek versus 70% for South Prong (**Table 2**).

Average DIN (nitrate + nitrite + ammonium) yields for Crane Creek were about double values for South Prong for both 2016 and 2017 (**Table 2** and **Figures 5G,H**). Annual yields of nitrate + nitrite averaged ∼2.6 times greater for Crane Creek than South Prong (**Table 2**). In contrast, ammonium yields were the same in both basins in 2016 and 44% higher for Crane Creek

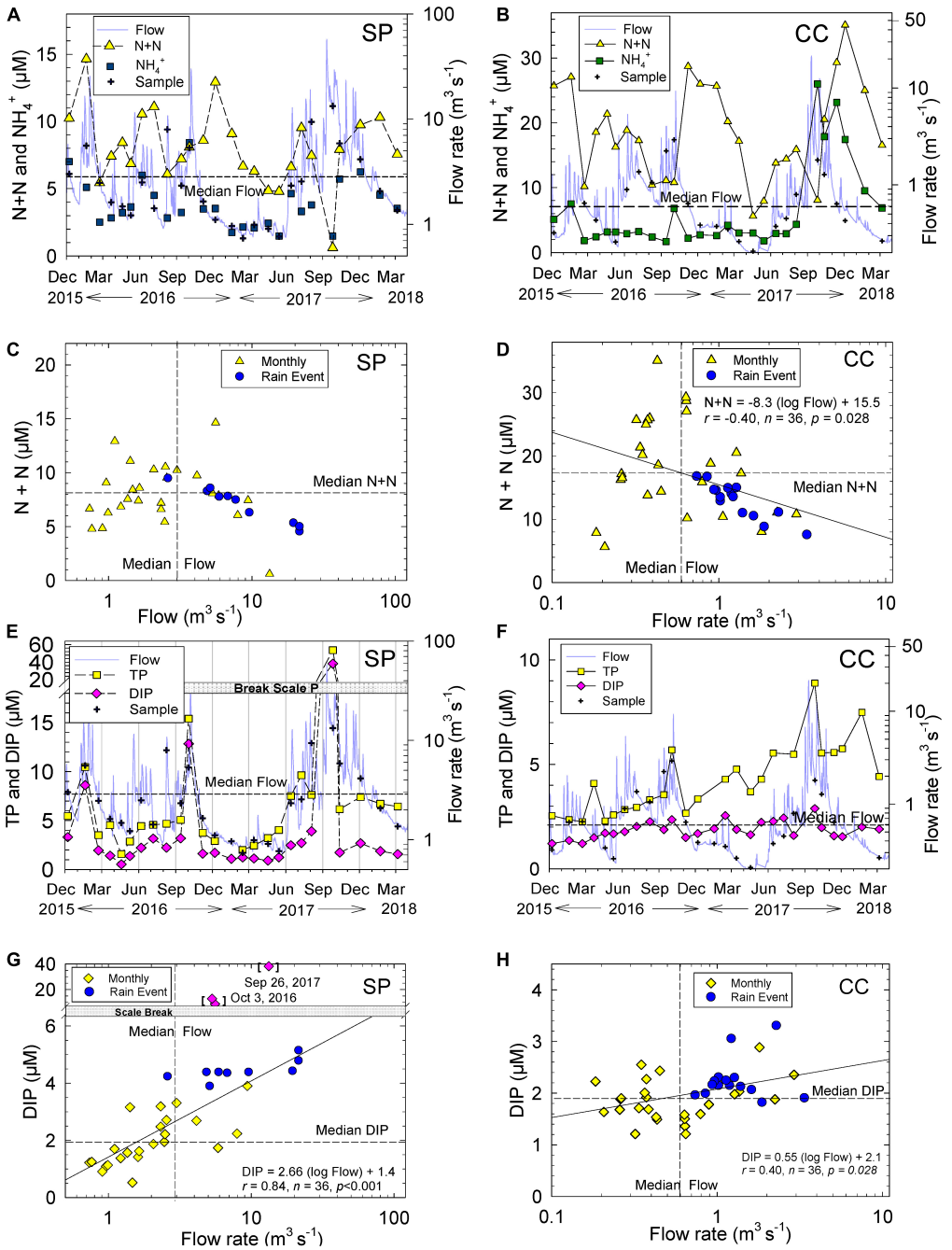

FIGURE 4 | Nitrate + Nitrite (N + N), ammonium (NH_4^+) and flow rate for monthly samples from **(A)** South Prong Saint Sebastian River (SP) and **(B)** Crane Creek (CC). N + N versus flow rate for **(C)** SP and **(D)** CC. Total phosphorus (TP), dissolved inorganic P (DIP) and flow rate for **(E)** SP and **(F)** CC. DIP versus flow rate for **(G)** SP and **(H)** CC. Equations and lines for **(D,G,H)** (except data in parentheses) from linear regression, correlation coefficient (*r*), number samples (*n*) and *p* statistic.

in 2017. PN accounted for 15-24% of TN yield for the two IRL tributaries (**Table 2**).

Average annual yields of DIP and particulate P for South Prong were higher than those for Crane Creek (**Table 2**). In contrast, yields for DOP were higher for Crane Creek (**Table 2**). However, particulate P comprised only ∼28% of the TP flux to the IRL relative 76% for global rivers.

Total suspended solids yields from South Prong averaged 27% greater than for Crane Creek (**Table 2**) because of higher TSS concentrations and greater increases in TSS with increased flow in South Prong. TSS values in both tributaries were very low; therefore, yields for TSS for both tributaries were only 3-5% of fluxes for world rivers (**Table 2**). Yet, we now know that IRL suspended matter was rich in C, N, and P.

TABLE 2 | Annual fluxes (tons y^{-1}) and yields (kg km^{-2} y^{-1}) for total nitrogen (TN), dissolved organic N (DON), nitrate + nitrite (N + N), ammonium (NH_4^+), dissolved inorganic N (DIN), particulate N (PN), total phosphorus (TP), dissolved inorganic P (DIP), dissolved organic P (DOP), particulate P (PP), dissolved organic carbon (DOC), particulate organic C (POC) and total suspended solids (TSS) to the Indian River Lagoon (IRL) during 2016 and 2017 from South Prong Saint Sebastian River (SP), Crane Creek (CC) and average global rivers.

Parameter	Year	SP	CC	SP	CC	Global*
		Flux (tons y^{-1})		Yield (kg km^{-2} y^{-1})		
TN	2016	106	25.1	729	770	483
	2017	171	29.0	1170	890	
DON	2016	70.4	11.9	482	365	121
	2017	127	13.2	870	405	
N + N	2016	11.4	7.1	78	218	–
	2017	13.8	7.3	94	224	
NH_4^+	2016	4.9	1.1	34	34	–
	2017	5.0	1.6	34	49	
DIN	2016	16.3	8.2	112	252	212
	2017	18.8	8.9	129	273	
PN	2016	19.7	5.0	135	153	152
	2017	25.2	6.9	172	212	
TP	2016	16.7	3.1	114	84	97
	2017	30.2	5.0	207	153	
DIP	2016	9.7	1.9	66	46	15.7
	2017	17.8	2.2	122	67	
DOP	2016	1.4	0.4	10	12	6.7
	2017	3.7	1.6	25	49	
PP	2016	5.6	0.84	38	26	74.2
	2017	8.7	1.2	60	37	
DOC	2016	1760	316	12,100	9,700	1840
	2017	3190	381	21,800	11,700	
POC	2016	227	16.4	1,550	500	1570
	2017	431	19.2	2,950	590	
TSS	2016	820	147	5,620	4,500	142,000
	2017	1130	195	7,740	6,000	
–	–	10^6 m^3 y^{-1}		10^5 m^3 km^{-2} y^{-1}		
Runoff	2016	99.3	28.3	6.8	8.7	4.2
	2017	147	31.4	10.1	9.6	
Rainfall	2016	236	54.1	16.2	16.6	–
	2017	309	57.7	21.2	17.7	

Seitzinger et al. (2010) and Berner and Berner (2012). Earth's hydrologically active drainage area = 89 × 10^6 km^2 (Stallard, 1998).

Post-hurricane Surveys of Indian River Lagoon

Data from monthly surveys by St. Johns River Water Management District [SJRWMD] (2020b) were used to investigate changes in water chemistry in the IRL following Hurricane Irma. Salinity at 10 stations throughout Central IRL, North IRL and BRL decreased from an average of 34 ± 3 in July-August 2017 to <20 in September-October 2017 following the hurricane (**Figures 1**, **6A**). The lowest salinities of 14-17 occurred during October 2017 at each of four IRL stations located near tributaries to the IRL: station 21 (Eau Gallie River), station 23 (Crane Creek), station 24 (Turkey Creek) and station 28 (South Prong) (**Figures 1**, **6A**). Salinity subsequently increased over time with some spatial variations (**Figure 6A**). Water temperatures in the IRL were >25°C during September-November 2017 and again after April 2018; lowest temperatures during January 2018 were 15-17°C (**Figure 6B**).

Concentrations of DIN increased from <5 μM to >20μM during October-December 2017 at all IRL stations except 28 (**Figure 6C**). Highest DIN values of 50-60 μM were obtained at northern stations 13 and 16, whereas values of 26-35 μM were recorded at stations 21, 23, and 24, adjacent to tributaries (**Figure 6C**). Average concentrations of DOC and DON also increased from 600 to > 1,000 μM and ∼30 to ∼50 μM, respectively, at IRL stations near tributaries following rainfall during fall 2017 (**Figures 6E,F**). Following larges fluxes of DIN, DOC, and DON to IRL, concentrations of chlorophyll *a* increased to >40 μg/L, beginning as early as October 2017 at station 24, near Turkey Creek (**Figure 6D**). Corresponding data for the biomass of *Aureoumbra lagunensis* and other nanoeukaryotes showed the onset of a bloom in December 2017-January 2018 (**Figures 7A,B**).

Concentrations of chlorophyll *a* remained high from January to May 2018 (**Figure 6D**), with cell counts often > 1 × 10^6 per mL (Judice et al., 2020; Phlips et al., 2021). The nanoeukaryotic bloom peaked during January-April 2018 (**Figures 7A,B**). Concentrations of TSS during the bloom ranged from 16 to 24 mg L^{-1} (**Figure 7C**). Salinity decreased to 15-20 during late spring and summer 2018 when concentrations of dissolved inorganic N and P were low and DOP values were decreasing (**Figures 6**, **7**; St. Johns River Water Management District [SJRWMD], 2020b). During the same period, concentrations of chlorophyll *a* and phytoplankton biomass diminished (**Figures 6D**, **7A,B**).

DISCUSSION

Drainage Basin Controls on Nutrient Fluxes to the Indian River Lagoon

The Variables

Differences in topography, climate, land use, soil type and water flow rate create a myriad of possible variables that control concentrations and fluxes of N and P species from tributaries and outfalls to estuaries (Pellerin et al., 2006; Chen et al., 2015; Bussi et al., 2017). The South Prong, Crane Creek and other IRL drainage basins have essentially the same topography and sub-tropical climate. Therefore, similarities and differences in nutrient concentrations and fluxes from IRL tributraries are discussed here based on land use, soil type and flow rate. Successful management of stormwater depends on knowing how drainage basins and estuaries might respond to future changes in variables that control concentrations and fluxes of nutrient species.

As detailed previously, South Prong flows through mainly agricultural, forested and open land whereas Crane Creek traverses mainly residential-commercial land (Gao and Rhew, 2013). Impervious land area was estimated at 3-5% and 32-37%

for the South Prong and Crane Creek basins, respectively (Gao and Rhew, 2013; Harper and Baker, 2013). Agricultural use in the South Prong drainage basin was almost evenly divided between citrus groves and pasture for cattle ranching. Most citrus groves were located west of Ten Mile Ridge and Highway I-95 in the westernmost portion of the South Prong drainage basin where there is active water control and retention. No heavy industry was present in either drainage basin. The Crane Creek drainage basin contained <0.5% of >50,000 septic systems along the IRL in Brevard County; the South Prong drainage basin contained ∼20% of >30,000 septic systems in Indian River County (Gao and Rhew, 2013; Harper and Baker, 2013).

Area soils are mostly Spodosols, sandy soils on flatwood landscapes that include saw palmetto fields and piney woods that can have organic-rich deeper layers (Harris et al., 2010). These soils have a low sorption capacity for nitrate and phosphate; therefore, nutrients applied to such soils may runoff into tributaries without proper soil management (Harris et al., 2010). Soils also are classified in Hydrologic Soil Groups defined based on soil texture and runoff potential from low (A) to high (D) runoff (United States Department of Agriculture, 2009). Soil types in the Crane Creek drainage basin were 50% A/D (>90% sand, <10% clay) and 40% B/D (50-90% sand and 10-20% clay). Dual classification (i.e., combined with D) is used unless soils in a specific area are adequately drained (Harper and Baker, 2013). Soils in the South Prong basin were 37% A/D and 51% C/D (<50% sand and 20% clay and/or organic matter) with higher runoff potential unless drained. In short, soils in the South Prong basin were thicker and less sandy with a greater reservoir of clay and organic matter (Wettstein et al., 1987). Additionally, the Crane Creek drainage basin had much greater turfgrass (sod) coverage in residential–commercial areas and South Prong was more prone to flooding (Harper and Baker, 2013).

Flow rates in rivers and streams are the product of rainfall and processes that control runoff through drainage basins. Rainfall in both tributaries during 2017 was ∼50% greater than the 30-year average and double the average of 100 cm for global river basins (Berner and Berner, 2012). Annual water yield was greater for Crane Creek in 2016 because of its higher fraction of impervious surfaces and greater for South Prong in 2017 because of greater rainfall (**Table 2** and **Figure 2**). Runoff ratios (runoff divided by rainfall in the drainage basin) for Crane Creek were 0.52 in 2016 and 0.55 in 2017, an average of ∼22% higher than 0.42 in 2016 and 0.48 in 2017 for South Prong, likely due to the impact of more impervious surfaces in the Crane Creek basin.

Concentrations and Fluxes of Nitrogen and Phosphorus Species

Three different drainage-basin controls on nutrient concentrations and fluxes to the IRL are listed here and discussed in more detail below. Each of the following controls is influenced by land use, soil type and flow rate: (1) larger yields of DON were flushed through thicker layers of soil with a larger reservoir of organic matter during high water flow (South Prong) than through thin layers of turfgrass overlying sand (Crane Creek), (2) higher yields of dissolved inorganic P (DIP) were released from more P-rich soils that were subjected to biogeochemical processes linked to drought, excess rainfall and flooding in 2017 (South Prong) than from turfgrass blanketing well-drained sand with an overall lower P content (Crane Creek) and (3) a greater yield of dissolved inorganic N (DIN) was exported to the IRL from fertilized turfgrass, plus runoff of reclaimed water used for lawn irrigation (Crane Creek) than from land with 75% less turfgrass and limited reclaimed water (South Prong).

Median concentrations of DON in South Prong and Crane Creek (**Table 1**) were similar to values of ∼35 μM in the C-24 Canal that empties into St. Lucie Estuary and then the Southern IRL (Li et al., 2016). DON in these three Florida tributaries were 67% higher than 21 μM for global rivers (Seitzinger et al., 2010). Above average runoff, a subtropical climate, as well as upland agricultural and other human activities, support high DON values in IRL tributaries. High DON concentrations were cited as important to sustaining blooms of *Aureoumbra lagunensis* in Baffin Bay, Texas (Cira and Wetz, 2019).

Despite similar median values for DON in the two Central IRL tributaries, concentrations of DON in South Prong increased by a factor of ∼2 when flow rates increased by 10-fold (**Figure 3G**). No similar trend was observed for the more quickly drained Crane Creek soils with a smaller reservoir of soil organic matter (**Figure 3H**). The % of TN that was DON in South Prong increased from 56% during monthly surveys to 74% during high water flow; no change was observed in Crane Creek as the % of TN that was DON remained at 48 ± 11%. A similarly lower % DON has commonly been reported in tributaries flowing through more urban settings during rain events (Aitkenhead-Peterson et al., 2009).

High yields for DON from South Prong than Crane Creek during both 2016 and 2017 may be linked to soil cover (**Table 2** and **Figures 5E,F**). The South Prong drainage basin includes more open land, saw palmetto fields, mature citrus groves, and limited residential-commercial property relative to much more turfgrass and impervious surfaces in Crane Creek. Previous studies have found a lower reservoir of organic matter in residential lawns because thin (<20 cm) layers of turfgrass often cover soil amended by importing C- and N-poor, sand (Peach et al., 2019). This turfgrass scenario was common in our study area. Thicker (>60 cm) soil layers were found in the South Prong basin because of fourfold lower residential land use (Wettstein et al., 1987). DON has been widely found to be well flushed from organic-rich upper soil horizons during high flow and flooding (Martin and Harrison, 2011; Li et al., 2016). Increased oxidation and remineralization of organic matter occurred in both basins in 2017 because redox potentials likely increased during the 6 months of drought (Dierberg et al., 2012). However, these conditions had a greater impact on the larger reservoir of organic matter in soils of the South Prong basin because the September and October 2017 rains flooded the more slowly drained soils and subsequently solubilized more organic matter and created a larger flux of DON. Yields for DOC for the South Prong versus Crane Creek drainage basins followed the same pattern as DON for the same reasons (**Table 2**).

Yields for DIP from South Prong averaged ∼60% higher than for Crane Creek (**Table 2**). This difference also can be linked to biogeochemical processes in thicker, more P-rich soil versus

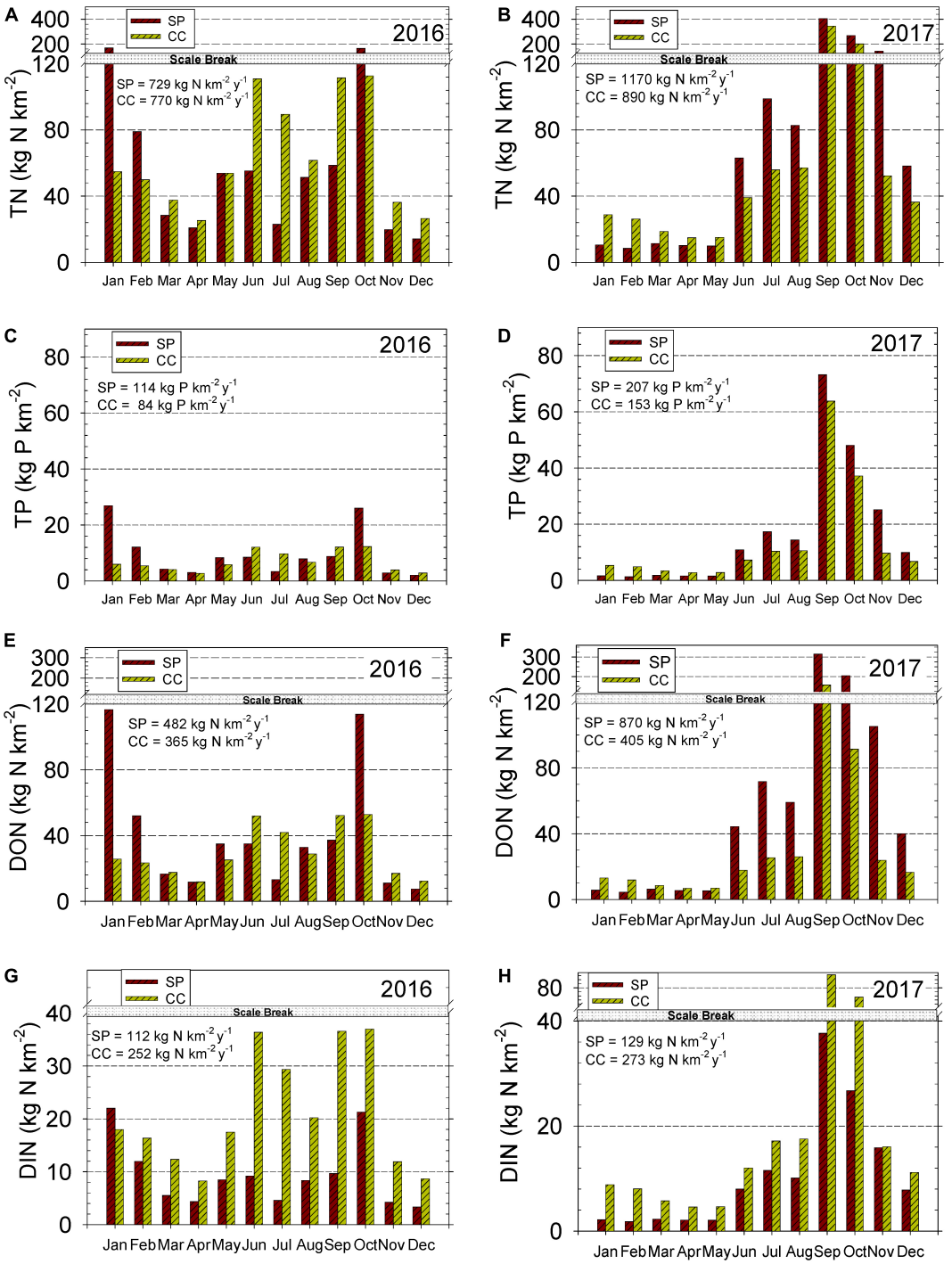

FIGURE 5 | Yields from South Prong Saint Sebastian River (SP) and Crane Creek (CC) to the Indian River Lagoon (IRL) during 2016 and 2017 for **(A,B)** total nitrogen (TN), **(C,D)** total phosphorus (TP), **(E,F)** dissolved organic N (DON), and **(G,H)** dissolved inorganic N (DIN). Totals for each year shown on upper left of graphs.

turfgrass, especially during drought and flood conditions of 2017. Previous studies in a stormwater treatment area in Florida showed that long droughts induced oxidation of organic matter and removal of P *via* adsorption or by precipitation with Ca- and Fe- bearing minerals (Dierberg et al., 2012). Phosphorus was later released after soil was inundated for weeks to months, thereby creating reducing, sometimes anoxic, conditions. In the turfgrass-rich Crane Creek drainage basin, releases of P were likely constrained by underlying P-deficient sandy soil, a ban on P in fertilizer for turfgrass, and lower water retention times

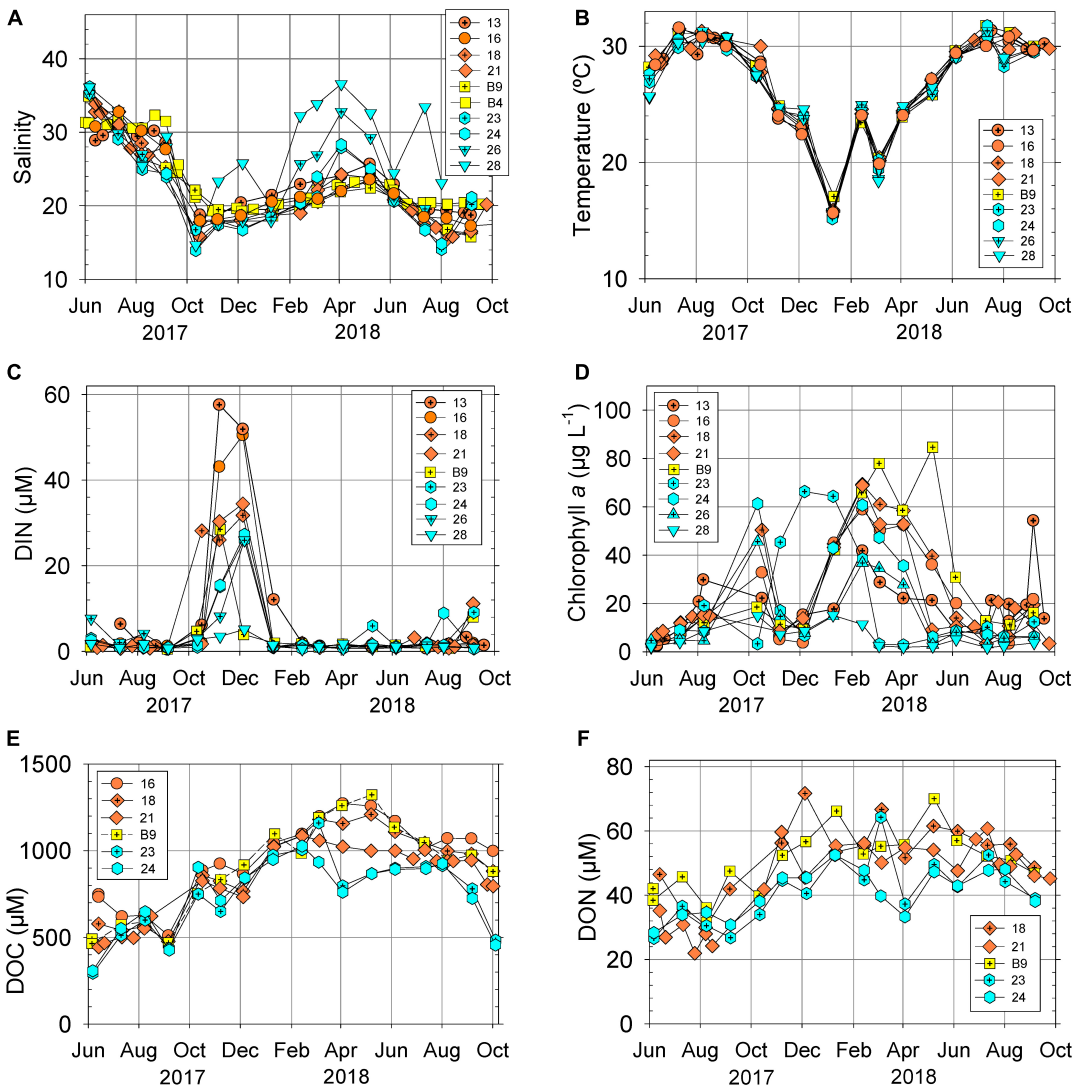

FIGURE 6 | (A) Salinity, **(B)** temperature, **(C)** dissolved inorganic nitrogen (DIN), **(D)** chlorophyll *a*, **(E)** dissolved organic carbon (DOC) and **(F)** dissolved organic N (DON) for stations in the Indian River Lagoon (IRL) and Banana River Lagoon (BRL). Data from St. Johns River Water Management District [SJRWMD] (2020b). Markers are color coded as orange (North IRL), yellow (BRL) and blue (Central IRL).

in Crane Creek than in the South Prong basin. Therefore, a fivefold lower slope for DIP versus flow rate was found for Crane Creek (**Figures 4G,H**). Even with different pH values in each tributary and basin (**Table 1**), differences in desorption of phosphate between tributaries were likely small (Morris and Hesterberg, 2010); there was just less available phosphorus in the Crane Creek basin. Therefore, the most important factor supporting the very high flux of DIP *via* South Prong in 2017 was more available P and organic matter, plus the combined effects of drought and flooding.

Distinctly different results were found for DIN than for DON and DIP. Concentrations and yields of DIN for the Crane Creek drainage basin were greater than twofold higher than values for South Prong (**Table 2** and **Figures 5G,H**). Typical concentrations of DIN in Crane Creek were 15-40 µM (**Figure 4B**) with an average of 37% of TN present as DIN. In contrast, values for DIN in South Prong were 5-15 µM, with an average of 19% of TN present as DIN. Very low DIN concentrations (<2 µM) were found at high flow in South Prong (**Figure 4A**). Higher DIN values for Crane Creek can be explained by the larger fraction of land area with irrigated and N-fertilized turfgrass and residential vegetation plus releases of N-rich reclaimed water (Harper and Baker, 2013). Reclaimed water that we collected from the irrigation system at the Crane Creek Reserve Golf course contained ∼640 µM nitrate + nitrite and 190 µM ammonium. The golf course is situated ∼1 km upstream from the USGS flow gauge. Melbourne, Florida, recycles an average of ∼8 million liters of reclaimed water for irrigation per day (City of Melbourne, 2021). Therefore, ∼34 t y^{-1} of TN could runoff into the combined Melbourne drainage basins of Crane Creek and

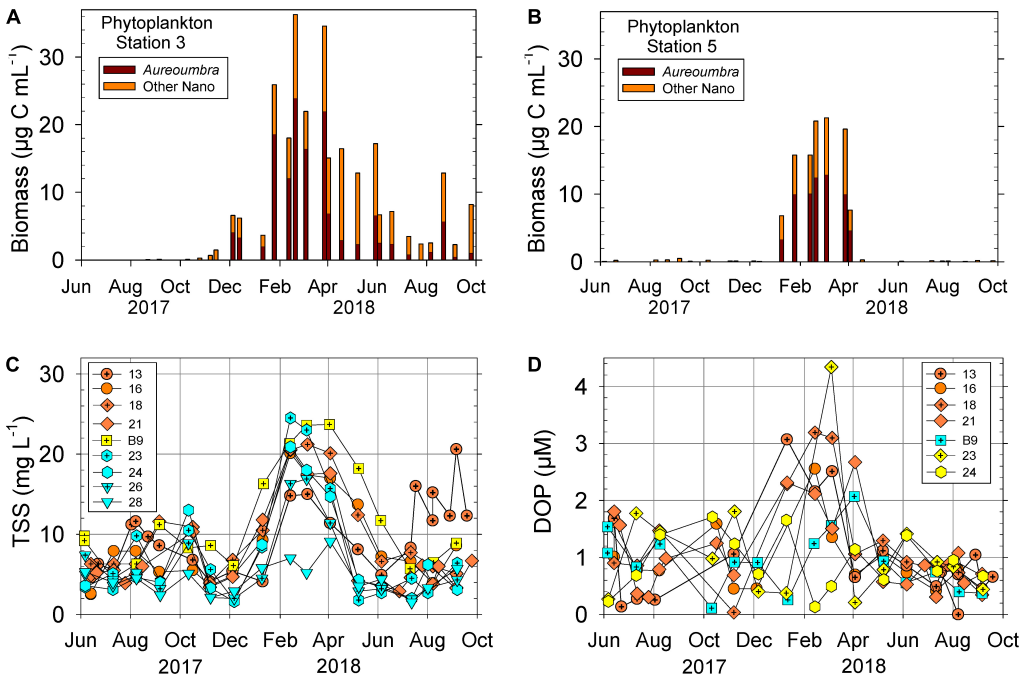

FIGURE 7 | Phytoplankton biomass for *Aureoumbra lagunensis* and other nanoeukaryotes at plankton stations **(A)** 3 and **(B)** 5 (**Figure 1**). **(C)** Total suspended solids (TSS) and **(D)** dissolved organic phosphorus (DOP) for stations in the Indian River Lagoon (IRL) and Banana River Lagoon (BRL). Data for plankton from Phlips et al. (2021) and physicochemical parameters from St. Johns River Water Management District [SJRWMD] (2020b). Markers for **(C,D)** are color coded as orange (North IRL), yellow (BRL) and blue (Central IRL).

Eau Gallie River. Based on ∼25% runoff of reclaimed water (Tetra Tech Inc and Closewaters LLC, 2021), ∼8.5 t y^{-1} of N could be carried toward the lagoon, relative to average TN fluxes of 27 t y^{-1} from Crane Creek (**Table 2**) + 12 t y^{-1} from Eau Gallie River (**Supplementary Table 3**). This amounts to ∼22% of the TN flux. Plans for ≥50% decreases in N and P concentrations in reclaimed water are being implemented in Brevard County, Florida.

Nutrient fluxes from Turkey Creek and Eau Gallie River corroborate controls discussed above for South Prong and Crane Creek. For example, DON yields for Turkey Creek and Eau Gallie River were 27-66% lower than for South Prong and were similar or less than observed for Crane Creek (**Table 2** and **Supplementary Table 3**). Therefore, trends for Turkey Creek and the Eau Gallie River were consistent with Crane Creek, all showing that thin layers of turfgrass over sand in residential areas had less solubilization and runoff of DON. Yields for DIP from the Turkey Creek basin in 2017 were lower than for Crane Creek and much lower than for South Prong; DIP yields from Eau Gallie River more closely matched those for Crane Creek (**Table 2** and **Supplementary Table 3**). Such trends further support a lower yield of DIP from residential lands with turfgrass cover and bans on P fertilizer than more undeveloped land containing a larger reservoir of phosphorus and organic matter. The DIN yield during 2017 for Turkey Creek averaged 70% lower than for Crane Creek; whereas the DIN yield for Eau Gallie River in 2017 was only ∼12% less than for Crane Creek (**Table 2**). Similar DIN yields for Crane Creek and Eau Gallie River support impacts from more abundant residential land with fertilized turfgrass. The Turkey Creek drainage basin, with >20,000 septic systems, had a much lower DIN yield than Crane Creek (**Table 2** and **Supplementary Table 3**). This observation for Turkey Creek can be partly explained by significant water diversion to the west plus water retention areas in wetlands. Additional sources of DIN to the IRL, north of the tributaries that we studied, likely include groundwater, sewer overflows, reclaimed water, leakage from septic systems and benthic fluxes of ammonium from fine-grained, organic-rich sediments (Lapointe et al., 2015, 2020; Barile, 2018; Fox and Trefry, 2018; Tetra Tech Inc and Closewaters LLC, 2021). The relative importance of these potential sources of N is not well quantified for the IRL.

Consequences of Stormwater Runoff to the Indian River Lagoon

Stormwater inputs of freshwater and nutrients can be trapped behind the barrier islands of the IRL for weeks to months (Steward et al., 2005; Rosario-Llantin and Zarillo, 2021), thereby promoting intense HABs, including an *Aureoumbra lagunensis* bloom in 2017-2018 (Galimany et al., 2020; Judice et al., 2020). Lapointe et al. (2020) highlighted the importance of land-based nutrients as a driving force for eutrophication and HABs in the IRL, especially noting a significant negative correlation between DIN and salinity. Furthermore, high TDN:TDP ratios (i.e., >70) in the IRL favored *Aureoumbra lagunensis* that can form dense blooms at low concentrations of TDP (Kang et al., 2015; Lapointe et al., 2020). Paerl et al. (2001) showed that stormwater

input during three sequential hurricanes delivered at least half the annual N load to Pamlico Sound, subsequently promoting three to fivefold increases in chlorophyll *a* for 5-6 months. Predicting and tracking flow rates, concentrations and ratios of pertinent nutrient species in IRL tributaries may foreshadow pending increases in chlorophyll *a* and HABs, thereby initiating or supporting appropriate responses.

As previously mentioned, Hurricane Irma was a major event during our study. It brought rain and flooding that began in early September 2017 and continued episodically through October 2017 (**Figures 2C,D**). In these 2 months of 2017, >50% of the annual fluxes of freshwater and ∼60% of annual fluxes of TN, and TP were transported to the IRL from South Prong, Crane Creek and other tributaries and outfalls to the IRL (**Figures 2**, **5**; Trefry et al., 2019). By comparison, <30% of the annual fluxes of freshwater, TN and TP were exported to the IRL from South Prong, Crane Creek and other tributaries during September and October 2016 (**Figures 2**, **5**; Trefry et al., 2019).

Freshwater runoff (salinity ∼0.1) during fall 2017 caused salinity to decrease from 34 to <20 and diluted lagoon water by at least 40% [((34–20)/34)*100]. Salinity <20 persisted from <1 to 4 months at the 10 stations (**Figure 6A**). Subsequent increases in salinity over time varied considerably, consistent with flushing times (R_{50} = 50% renewal time) that ranged from as low as ∼10 days in parts of Central IRL to as high as ∼100 days in the North IRL and >150 days in BRL (Steward et al., 2005; Rosario-Llantin and Zarillo, 2021). For example, salinity increased to ∼24 in less than 1 month and to 36 by April 2018 at station 28, near Sebastian Inlet that connects IRL to the Atlantic Ocean (**Figure 6A**). Salinities at stations 23, 24, and 26, located ∼20-30 km north of Sebastian Inlet remained below 18 until at least January 2018 (**Figure 6A**). All stations had salinities >20 by February-March 2018.

A negative relationship for DIN versus salinity in the IRL was observed following inputs of freshwater and DIN from Hurricane Irma (**Figures 6A,C**), confirming results by Lapointe et al. (2020). DIN values at IRL stations 13 and 16 were equal to or greater than a maximum of 52 μM in Crane Creek. Such high DIN concentrations in the IRL were not likely supported by tributaries such as Crane Creek and South Prong because incoming freshwater accounted for only ∼40% of the water in the lagoon during late 2017 (**Figure 6A**). This observation supports previously discussed sources of DIN to the IRL, north of stations 18 and B9, that likely included groundwater, sewer overflows, leakage from septic systems and benthic fluxes of ammonium (Lapointe et al., 2015, 2020; Barile, 2018; Fox and Trefry, 2018; Tetra Tech Inc and Closewaters LLC, 2021).

Ammonium accounted for an average of 60% of DIN in the IRL during the period of peak DIN concentrations, consistent with an average 64 ± 21% of DIN as ammonium in the IRL for 2015-2018 (St. Johns River Water Management District [SJRWMD], 2020b). Ammonium concentrations in nearby Crane Creek were ≥50% of values for DIN during high flow in fall 2017. This fraction of DIN that was ammonium in Crane Creek during high flow was much greater than monthly averages of 22% for Crane Creek and 30% for South Prong. Enhanced ammonium in the IRL tributaries during high flow and flooding (**Figures 4A,B**) was likely due to lower redox potentials in the drainage basins. Most importantly, the large fraction of DIN that was ammonium in the IRL and the tributaries during very high flow was especially favorable for *Aureoumbra lagunensis*, an organism that is unable to use nitrate as source of N (Deyoe and Suttle, 1994). In addition to DIN, concentrations of DOC and DON increased in the lagoon between September 2017 and January 2018 (**Figures 6E,F**).

As salinity increased, concentrations of chlorophyll *a* and phytoplankton biomass increased (**Figures 6A,D**, **7A,B**). Increases in chlorophyll *a* and the onset of a eukaryotic bloom began as early as October 2017, but lagged into February 2018 at some stations until salinities eventually increased to >20 (Phlips et al., 2021; **Figures 6A,D**, **7A,B**). Previous laboratory studies showed that specific growth rates for *Aureoumbra lagunensis* slowed considerably at salinities of 10 and 15; however, specific growth rates at 25°C were not significantly different for salinities of 20-50 (Buskey et al., 1998). Water temperature in the IRL was favorable (>25°C), except during January and March, 2018 (**Figure 6B**). The bloom varied in intensity and duration in the North IRL and BRL (**Figures 7A,B**; Phlips et al., 2021). Biomass for *Aureoumbra lagunensis* plus other nanoeurkaryotes accounted for an average of 90 and 97% of total phytoplankton biomass, respectively, at phytoplankton stations 3 and 5 during the months of active blooms (December-May 2018; **Figures 7A,B**). Lower chlorophyll *a* was found at northern stations 13 and 16 as well as southern stations 26 and 28 (**Figure 6D**). Variations in chlorophyll *a* and phytoplankton biomass likely reflected variations in salinity and temperature. Continuous data for salinity and chlorophyll *a* obtained only for station B4 showed reasonably good correspondence with results from monthly surveys (St. Johns River Water Management District [SJRWMD], 2020a).

Several shifts in concentrations of nutrient species occurred during the bloom (January-May 2018). For example, concentrations of DIN decreased to <2 μM by January 2018 and remained low at all stations, except for a spike in April-May 2018 (**Figure 6C**) that was predominantly ammonium (St. Johns River Water Management District [SJRWMD], 2020b). This 2018 spike for DIN was probably related to benthic fluxes or recycling of organic N in the water column or at the sediment-water interface. The overall deficiency in DIN during the bloom likely led to uptake of components of DON, such as urea and amino acids, to support primary productivity (Kang et al., 2015; Cira and Wetz, 2019). DON in the IRL typically accounts for 80 to >90% of the TDN (Lapointe et al., 2020); but, during the bloom, DON comprised an average of 98% of TN, except for localized and short-term increases in DIN (**Figure 6C**; St. Johns River Water Management District [SJRWMD], 2020b).

Concentrations of DON and DOP varied considerably during the bloom (**Figures 6F**, **7D**), likely resulting from cycles of assimilation and release of these species (Kang et al., 2015; Cira and Wetz, 2019). Concentrations of DOP decreased appreciably during April 2018, likely due to consistent uptake by *Aureoumbra* (**Figure 7D**). Ratios for TDN:TDP were as high as 100 (St. Johns River Water Management District [SJRWMD], 2020b); however, these totals do not accurately assess the bioavailable

fractions of DON and DOP. Ratios for DIN:DIP were constrained by very low values for DIP, but were likely much >100 (St. Johns River Water Management District [SJRWMD], 2020b). Overall, decreases in salinity to 15-20 during late spring and summer 2018, along with low concentrations of inorganic N and P and decreasing DOP values, likely combined with biological processes to diminish the bloom by mid-2018 (**Figures 6**, **7**; St. Johns River Water Management District [SJRWMD], 2020b).

Concentrations of TSS during the bloom (**Figure 7C**) were at least 10 mg L^{-1} higher than typical values for the IRL (St. Johns River Water Management District [SJRWMD], 2020b). At 10 mg L^{-1}, the mass of excess TSS in 1 m^3 of water would be 10 g. For a 20 km × 2 km area (equivalent to an area in the IRL from stations 16 to 21) and a depth of 1 m, the estimated mass of TSS would be 400 t [(20,000 m × 2,000 m × 1 m) × (10 g m^{-3})] = 400 × 10^6 g = 400 t]. By comparison, annual fluxes of less organic-rich suspended matter from Crane Creek and South Prong averaged ∼170 t y^{-1} and 1000 t y^{-1}, respectively (**Table 2**). Therefore, decomposition of residual, organic-rich particles from the bloom provided a potentially large source of nutrients and a high biochemical oxygen demand in the IRL.

SYNTHESIS AND PERSPECTIVES

Data from our investigation showed that certain drainage basin characteristics, combined with extended drought and heavy rainfall, significantly increased tributary concentrations and fluxes of key N and P species to the IRL during fall 2017. This extreme runoff helped support a bloom of the brown tide alga *Aureoumbra lagunensis* as part of a nanoeukaryotic bloom that overran North IRL and BRL for ∼5 months of 2018 (**Figures 7A,B**). The events of 2017 also prompted concern for even larger nutrient fluxes in the future because storms with greater frequency and intensity have been predicted by scenarios for climate change (Trenberth and Asrar, 2014; Bhatia et al., 2019). We highlight here results from our study that contribute to an evolving synthesis of knowledge about the onset and decline of *Aureoumbra lagunensis* blooms. Then, we present a brief perspective on management and planning decisions for barrier island lagoons as we confront climate change and continued population growth.

A synthesis for reconstructing *Aureoumbra* blooms has progressed well since the 1990s and the 8-year plight in Laguna Madre, Texas (Buskey et al., 2001). Contributions to the synthesis were added after a 2013-2015 bloom in Baffin Bay, Texas (Cira and Wetz, 2019) and three separate blooms in the IRL between 2012 and 2018 (Kang et al., 2015; Phlips et al., 2015, 2021; Lapointe et al., 2020). Common physicochemical factors supporting this specific HAB in barrier island lagoons include poor flushing, large pulses of nutrients, high concentrations of DON and high use rates for recycled N; optimal growth occurs at temperatures >20°C, salinities of 20-50 and TDN:TDP ratios >20, but less than ∼70 (Liu et al., 2001; Kang et al., 2015; Cira and Wetz, 2019). The importance of grazing by zooplankton and other biological factors that significantly influenced *Aureoumbra* blooms have been described by others (Buskey et al., 2001; Kang et al., 2015; Phlips et al., 2015, 2021; Cira and Wetz, 2019).

We showed that extreme concentrations and fluxes of some nutrient species to the IRL during high flow, especially DIN, DON and DIP, were linked to extreme rain, runoff and flooding associated with Hurricane Irma in 2017. During high flow in 2017, ∼50% of DIN in tributaries was ammonium, a more favorable species for growth of *Aureoumbra lagunensis* (**Figures 6A,C**; Deyoe and Suttle, 1994; St. Johns River Water Management District [SJRWMD], 2020a). Inputs of these nutrient species helped support the 2017-2018 bloom. The impacts of salinity and temperature in our IRL study seemed consistent with laboratory results for specific growth rates by Buskey et al. (1998). Low salinity seems to have added a lag time and slowed the growth rate of *Aureoumbra* at the beginning of the 2017-2018 bloom in the IRL (**Figures 6A,D**, **7A,B**). Low concentrations of DIN and DIP were observed throughout the bloom. Although we did not experience hypersalinity during our study in the IRL, the impact of hypersalinity favoring growth of *Aureoumbra* was a factor in the 2012-2013 bloom in the IRL (Buskey et al., 2001; Kang et al., 2015; Cira and Wetz, 2019). The eventual decline of an *Aureoumbra* bloom seemed to require a sustained period wherein one or more of the following trends occurred: low salinity and/or temperature, a decrease in bioavailable DON and DOP, very low DIP, and biological processes.

Control of stormwater is perhaps the most cited management goal for estuaries, including barrier island lagoons (National Research Council, 2009). A massive effort and great expense have been invested in controlling nutrients in the IRL as well as estuaries across the United States and around the world (National Research Council, 2009; Romnée et al., 2015; Tetra Tech Inc and Closewaters LLC, 2021). There are many innovative and tested approaches for stormwater management that include engineering, land-use planning, and regulatory methodologies (National Research Council, 2009). The wide spectrum of research on stormwater has generated useful information and experiences that can often be applied elsewhere. Climate change and continued population growth further complicate planning for stormwater management.

Our study reinforced previous observations that concentrations of some chemical species of N and P carried by tributaries to estuaries, including IRL, increase when flow rates increase (Martin and Harrison, 2011: Chen et al., 2015; Jeanneau et al., 2015; Li et al., 2016). This trend favors increased nutrient fluxes during higher flow predicted to accompany climate change. In our investigation, we found higher yields for DON, DOC, and DIP where soil cover was thicker and had a higher reservoir of organic matter relative to areas with thin turfgrass layers overlying sand. Approaches to solving this stormwater problem in the IRL and similar basins include reducing, controlling and/or delaying runoff using techniques that are best suited for a given basin. Methods include building retention ponds and stormwater treatment areas, redirecting channels and ditches, diverting water inland, catching rain in barrels and cisterns and planting trees and shrubs (Tetra Tech Inc and Closewaters LLC, 2021). In most

cases, these efforts need to be carried out on a regional basis and include strategies that accommodate a range of possible extremes for runoff. Furthermore, backup for the most extreme events could include well-placed sites for short-term deep-well injection of stormwater, or other creative solutions.

We also encountered rather rapid flushing of DIN from turfgrass in residential drainage basins. In contrast with the DON and DIP, we did see a point whereafter concentrations of DIN decreased significantly during high flow (**Figures 4C,D**). In this second case, N-fertilizer is one target for stormwater management in some residential basins. Well-tested strategies for fertilizer control include the following: eliminate or reduce the amount of N-fertilizer applied, use well-tested slow-release fertilizers (Ivey et al., 2020), plant more trees, and try alternatives to turfgrass in at least portions of residential lands. For the IRL, shifting the start and end of the fertilizer ban 1 month later from the present period of June 1 to September 30 to July 1 to October 31 may better align the ban with recent rainfall data and seems worthy of consideration. For residential basins with large numbers of septic systems in the BRL and North IRL (Lapointe et al., 2015, 2020; Barile, 2018), solutions already implemented or in planning, include septic to sewer conversions, upgrades to existing septic systems and improvements to wastewater treatment facilities (National Research Council, 2009; Tetra Tech Inc and Closewaters LLC, 2021).

Tracking the success of stormwater management techniques is important. From a scientific perspective, data for TN and TP seem to have more limited value for managing nutrient inputs to estuaries because solutions to nutrient problems depend, in part, on knowing the specific chemical forms of N and P present. Data for major chemical species of N and P, as in this study, should prove to be more beneficial. However, acquiring data for specific organic molecules of N and P species and compound-specific stable N and C isotope data provide an even stronger database for identifying and managing specific sources of nutrient species. Additional high-resolution data from continuous sensors with more sophisticated chemical instrumentation are needed in tributaries to calculate and predict fluxes more accurately; they also provide a richer database for identifying future problems. There are many tools for controlling stormwater runoff. Careful monitoring and matching the solution to specific nutrient species in each drainage basin seem of the utmost importance.

DATA AVAILABILITY STATEMENT

The raw data supporting the conclusions of this article will be made available by the authors, without undue reservation.

AUTHOR CONTRIBUTIONS

Both authors listed have made a substantial, direct and intellectual contribution to the work, and approved it for publication.

FUNDING

Funding for this project was provided by the Florida Legislature as part of the Florida Department of Environmental Protection Grant Agreement No. NS005-Brevard County Muck Dredging. Publication of this article was funded in part by the Open Access Subvention Fund and the John H. Evans Library.

ACKNOWLEDGMENTS

We thank John Windsor of Florida of Technology (FIT) for his outstanding performance in the challenging role of Project Manager and for valuable scientific discussion and constructive criticism. Virginia Barker, Matt Culver, Mike McGarry, and Walker Dawson from the Brevard County Natural Resources Management Department were important contributors for logistics and background information; we also are most thankful for their keen interest and participation in this project. We thank Chuck Jacoby and Margie Lasi of SJRWMD for invaluable discussion regarding cycles for algae blooms and for updates on water diversion and other projects in the lagoon. Joel Steward of Dredging and Marine Consultants, LLC, graciously shared his wealth of knowledge on IRL. We thank Ed Phlips for sharing his plankton data and most helpful discussion. Stacey Fox, Bob Trocine, Jessica Voelker and Kate (Beckett) Fuller of FIT gave outstanding support in the field and laboratory. We greatly appreciate the support and encouragement of Frank Kinney of FIT and Thad Altman (Florida Legislature), who played important roles in guiding the project to fruition. Very helpful reviews from two reviewers were greatly appreciated. We thank the late George Maul for his long-term support and for continually reminding us that it was the *Saint* Sebastian River.

SUPPLEMENTARY MATERIAL

The Supplementary Material for this article can be found online at: https://www.frontiersin.org/articles/10.3389/fmars.2021.752945/full#supplementary-material

REFERENCES

Aitkenhead-Peterson, J. A., Steele, M. K., Nahar, N., and Santhy, K. (2009). Dissolved organic carbon and nitrogen in urban and rural drainage basins of south-central Texas: land use and land management influences. *Biogeochemistry* 96, 119–129. doi: 10.1007/s10533-009-9348-2

Barile, P. J. (2018). Widespread sewage pollution of the Indian River Lagoon system, Florida (USA) resolved by spatial analyses of macroalgal biogeochemistry. *Mar. Pollut. Bull.* 128, 557–574. doi: 10.1016/j.marpolbul.2018.01.046

Bergman, M. J., Green, W., and Donnangelo, L. J. (2002). Calibration of storm loads in the South Prong drainage basin, using basins/HSPF. *J. Am. Water Resour. Assoc.* 38, 1423–1436. doi: 10.1111/j.1752-1688.2002.tb04356.x

Berner, E. K., and Berner, R. A. (2012). *Global Environment: Water, Air, and Geochemical Cycles*. Princeton: Princeton University Press.

Bhatia, K. T., Vecchi, G. A., Knutson, T. R., Murakami, H., Kossin, J., Dixon, K. W., et al. (2019). Recent increases in tropical cyclone intensification rates. *Nat. Commun.* 10:635. doi: 10.1038/s41467-019-08471-z

Björkman, K., and Karl, D. M. (1994). Bioavailability of inorganic and organic phosphorus compounds to natural assemblages of microorganisms in Hawaiian coastal waters. *Mar. Ecol. Prog. Ser.* 111, 265–273. doi: 10.3354/meps111265

Buskey, E. J., Hongbin, L., Collumb, C., Guilherme, J., and Bersano, F. (2001). The decline and recovery of a persistent Texas brown tide algal bloom in the Laguna Madre (Texas. USA). *Estuaries* 24, 337–346. doi: 10.2307/1353236

Buskey, E. J., Wysor, B., and Hyatt, C. (1998). The role of hypersalinity in the persistence of the Texas 'brown tide' in the Laguna Madre. *J. Plankton Res.* 20, 1553–1565. doi: 10.1093/plankt/20.8.1553

Bussi, G., Janes, V., Whitehead, P. G., Dadson, S. J., and Holman, I. P. (2017). Dynamic response of land use and river nutrient concentration to long-term climatic changes. *Sci. Total Environ.* 590–591, 818–831. doi: 10.1016/j.scitotenv.2017.03.069

Cangialosi, J. P., Latlo, A. S., and Berg, R. (2018). *Hurricane Irma (AL112017). National Hurricane Center Tropical Cyclone Report*. Available online at https://www.nhc.noaa.gov/data/tcr/AL112017_Irma.pdf (accessed June 10, 2021).

Chen, N., Wu, Y., Chen, Z., and Hong, H. (2015). Phosphorus export during storm events from a human perturbed drainage basin, southeast China: implications for coastal ecology. *Estuar. Coast. Shelf Sci.* 166, 178–188. doi: 10.1016/j.ecss.2015.03.023

Chen, Y.-C., Liu, J.-H., Kuo, J.-T., and Lin, C.-F. (2013). Estimation of phosphorus flux in rivers during flooding. *Environ. Monit. Assess.* 185, 5653–5672. doi: 10.1007/s10661-012-2974-5

Cira, E. K., and Wetz, M. S. (2019). Spatial-temporal distribution of *Aureoumbra lagunensis* ("brown tide") in Baffin Bay. Texas. *Harmful Algae* 89:101669. doi: 10.1016/j.hal.2019.101669

City of Melbourne (2021). *Reclaimed Water*. Available online at https://www.melbourneflorida.org/departments/public-works-utilities/reclaimed-water (accessed June 10, 2021).

Cunningham, M. A., O'Reilly, C. M., Menking, K. M., Gillikin, D. P., Smith, K. C., Foley, C. M., et al. (2009). The suburban stream syndrome: evaluating land use and stream impairments in the suburbs. *Phys. Geogr.* 30, 269–284. doi: 10.2747/0272-3646.30.3.269

Deyoe, H. R., and Suttle, C. A. (1994). The inability of the Texas "brown" tide alga to use nitrate and the role of nitrogen in the initiation of a persistent bloom of this organism. *J. Phycol.* 30, 800–806. doi: 10.1111/j.0022-3546.1994.00800-x

Diaz, J. M., Holland, A., Sanders, J. G., Bulski, K., Mollett, D., Chou, C.-W., et al. (2018). Dissolved organic phosphorus utilization by phytoplankton reveals preferential degradation of polyphosphates over phosphomonoesters. *Front. Mar. Sci.* 5:380. doi: 10.3389/fmars.2018.00380

Diaz, R. J., and Rosenberg, R. (2008). Spreading dead zones and consequences for marine ecosystems. *Science* 321, 926–929. doi: 10.1126/science.1156401

Dierberg, F. E. (1991). Non-point source loadings of nutrients and dissolved organic carbon from an agricultural-suburban watershed in east central Florida. *Wat. Res.* 25, 363–374. doi: 10.1016/0043-1354(91)90073-y

Dierberg, F. E., DeBusk, T. A., Henry, J. L., Jackson, S. D., Galloway, S., and Gabriel, M. L. (2012). Temporal and spatial patterns of internal phosphorus recycling in a South Florida (USA) stormwater treatment area. *J. Environ. Qual.* 41, 1661–1673. doi: 10.2134/jeq2011.0448

Duncan, J. M., Welty, C., Kemper, J. T., Groffman, P. M., and Band, L. E. (2017). Dynamics of nitrate concentration-discharge patterns in an urban drainage basin. *Water Resour. Res.* 53, 7349–7365. doi: 10.1002/2017WR020500

Feng, S., Zhang, L., Wang, S., Nadykto, A. B., Xu, Y., Shi, Q., et al. (2016). Characterization of dissolved organic nitrogen in wet deposition from Lake Erhai basin by using ultrahigh resolution FT-ICR mass spectrometry. *Chemosphere* 156, 438–445. doi: 10.1016/j.chemosphere.2016.04.039

Fox, A. L., and Trefry, J. H. (2018). Environmental dredging to remove fine-grained, organic-rich sediments and reduce inputs of nitrogen and phosphorus to a subtropical estuary. *Mar. Tech. Soc. J.* 52, 42–57. doi: 10.4031/mtsj.52.4.3

Galimany, E., Lunt, J., Freeman, C. J., Houk, J., Sauvage, T., Santos, L., et al. (2020). Bivalve feeding responses to microalgal bloom species in the Indian River Lagoon: the potential for top-down control. *Estuar. Coasts* 43, 1519–1537. doi: 10.1007/s12237-020-00746-9

Gao, X., and Rhew, K. (2013). *TMDL Report: Dissolved Oxygen and Nutrient TMDLs for Eight Tributary Segments of the Indian River Lagoon*. Tallahassee, FL: Florida Department of Environmental Protection.

Harper, H. H., and Baker, D. M. (2013). *) Refining the Indian River Lagoon TMDL–Technical Memorandum Report: Assessment and Evaluation of Model Input Parameters*. Melbourne, DL: Brevard County Natural Resources Management.

Harris, W. G., Chrysostome, M., Obreza, T. A., and Nair, V. D. (2010). Soil properties pertinent to horticulture in Florida. *HortTech* 20, 10–18. doi: 10.21273/horttech.20.1.10

Ivey, J. E., Wolny, J. L., Heil, C. A., Murasko, S. M., Brame, J. A., and Parks, A. A. (2020). Urea inputs drive picoplankton blooms in Sarasota Bay. Florida, U.S.A. *Water* 12, 2755. doi: 10.3390/w12102755

Jeanneau, L., Denis, M., Pierson-Wickmann, A.-C., Gruau, G., Lambert, T., and Petitjean, P. (2015). Sources of dissolved organic matter during storm and inter-storm conditions in a lowland headwater catchment: constraints from high-frequency molecular data. *Biogeosciences* 12, 4333–4343. doi: 10.5194/bg-12-4333-2015

Jordan, T. E., Weller, D. E., and Pelc, C. E. (2018). Effects of local watershed land use on water quality in mid-Atlantic coastal bays and subestuaries of the Chesapeake Bay. *Estuar. Coasts* 41(Suppl. 1), S38–S53. doi: 10.1007/s12237-017-0303-5

Judice, T. J., Widder, E. A., Falls, W. H., Avouris, D. M., Cristiano, D. J., and Ortiz, J. D. (2020). Field-validated detection of *Aureoumbra lagunensis* brown tide blooms in the Indian River Lagoon, Florida, using Sentinel-3A OLCI and ground-based hyperspectral spectroradiometers. *GeoHealth* 4:e2019GH000238. doi: 10.1029/2019GH000238

Kandasamy, S., and Nath, B. N. (2016). Perspectives on the terrestrial organic matter transport and burial along the land-deep-sea continuum: caveats in our understanding of biogeochemical processes and future needs. *Front. Mar. Sci.* 3:259. doi: 10.3389/fmars.2016.00259

Kang, Y., Koch, F., and Gobler, C. J. (2015). The interactive roles of nutrient loading and zooplankton grazing in facilitating the expansion of harmful algal blooms caused by the pelagophyte, *Aureoumbra lagunensis*, to the Indian River Lagoon, FL, USA. *Harmful Algae* 49, 162–173. doi: 10.1016/j.hal.2015.09.005

Kroening, S. E. (2004). *Streamflow and Water-Quality Characteristics at Selected Sites of the St. Johns River in Central Florida, 1933 to 2002*. Reston, VA: USGS. Scientific Investigations Report 2004-5177.

Labry, C., Youenou, A., Delmas, D., and Michelon, P. (2013). Addressing the measurement of particulate organic and inorganic phosphorus in estuarine and coastal waters. *Cont. Shelf Res.* 60, 28–37. doi: 10.1016/j.csr.2013.04.019

Lapointe, B. E., Herren, L. W., Brewton, R. A., and Alderman, P. K. (2020). Nutrient over-enrichment and light limitation in seagrass communities in the Indian River Lagoon, an urbanized subtropical estuary. *Sci. Total Environ.* 699:134068. doi: 10.1016/j.sci.totenv.2019.134068

Lapointe, B. E., Herren, L. W., Derbortoli, D. D., and Vogel, M. A. (2015). Evidence of sewage-driven eutrophication and harmful algal blooms in Florida's Indian River Lagoon. *Harmful Algae* 43, 82–102. doi: 10.1016/j.hal.2015.01.004

Li, L., He, Z., Li, Z., Zhang, S., Li, S., Yongshan, W., et al. (2016). Spatial and temporal variation of nitrogen concentration and speciation in runoff and storm water in the Indian River drainage basin. South Florida. *Environ. Sci. Pollut. Res.* 23, 19561–19569. doi: 10.1007/s11356-016-7125-z

Liu, H., Laws, E. A., Villareal, T. A., and Buskey, E. J. (2001). Nutrient-limited growth of *Aureoumbra lagunensis* (Pelagophyyceae), with implications for its capability to outgrow other phytoplankton species in phosphate-limited environments. *J. Phycol.* 37, 500–508. doi: 10.1046/j.1529-8817.2001.037004500.x

Lorite-Herrera, M., Hiscock, K., and Jiménez-Espinosa, R. (2009). Distribution of dissolved inorganic and organic nitrogen in river water and groundwater in an agriculturally-dominated catchment, South-east Spain. *Water Air Soil Poll* 198, 335–346. doi: 10.1007/s11270-008-9849-y

Martin, R. A., and Harrison, J. A. (2011). Effect of high flow events on in-stream dissolved organic nitrogen concentration. *Ecosystems* 14, 1328–1338. doi: 10.1007/s10021-011-9483-1

Meybeck, M., Laroche, L., Dürr, H. H., and Syvitski, J. P. M. (2003). Global variability of daily total suspended solids and their fluxes in rivers. *Global Planet. Change* 39, 65–93. doi: 10.1016/s0921-8181(03)00018-3

Michelou, V. K., Lomas, M. W., and Kirchman, D. L. (2011). Phosphate and adenosine-5'-triphosphate uptake by cyanobacteria and heterotrophic bacteria in the Sargasso Sea. *Limnol. Oceanogr.* 56, 323–332. doi: 10.4319/lo.2011.56.1.0323

Morris, A. J., and Hesterberg, D. (2010). "Mechanisms of phosphate dissolution from soil organic matter," in *19th World Congress of Soil Science, Soil Solutions for a Changing World*, eds R. Gilkes and N. Prakongkep (Vienna: International Union of Soil Scientists), 37–39.

National Oceanic and Atmospheric Administration [NOAA] (2020). *Monthly US Climate Reports*. Asheville, NC: National Centers for Environmental Information.

National Research Council (2009). *Urban Stormwater Management in the United States*. Washington, DC: The National Academies Press, doi: 10.17226/12465

O'Connor, D. J. (1976). The concentration of dissolved solids and river flow. *Water Res. Res.* 12, 279–294.

Oelsner, G. P., and Stets, E. G. (2019). Recent trends in nutrient and sediment loading to coastal areas of the conterminous U.S.: insights and global context. *Sci. Total Environ.* 654, 1225–1240. doi: 10.1016/j.scitotenv.2018.10.437

Osburn, C. L., Handsel, L. T., Peierls, B. L., and Paerl, H. W. (2016). Predicting sources of dissolved organic nitrogen to an estuary from an agro-urban coastal watershed. *Environ. Sci. Technol.* 50, 8473–8484. doi: 10.1021/acs.est.6b00053

Paerl, H. W., Bales, J. D., Ausley, L. W., Buzzelli, C. P., Crowder, L. B., Eby, L. A., et al. (2001). Ecosystem impacts of three sequential hurricanes (Dennis, Floyd, and Irene) on the United States' largest lagoonal estuary, Pamlico Sound, NC. *Proc. Natl. Acad. Sci. U.S.A.* 98, 5655–5660.

Paolini, J. (1995). Particulate organic carbon and nitrogen in the Orinoco River (Venezuela). *Biogeochemistry* 29, 59–70. doi: 10.1007/BF00002594

Peach, M. E., Ogden, L. A., Mora, E. A., and Friedland, A. J. (2019). Building houses and managing lawns could limit yard soil carbon for centuries. *Carbon Balance Manag.* 14:9. doi: 10.1186/s13021-019-0124-x

Pellerin, B. A., Kaushal, S. S., and McDowell, W. H. (2006). Does anthropogenic nitrogen enrichment increase organic nitrogen concentrations in runoff from forested and human-dominated drainage basins? *Ecosystems* 9, 852-864.

Phlips, E. J., Badylak, S., Lasi, M. A., Chamberlain, R., Green, W. C., Hall, L. M., et al. (2015). From red tides to green and brown tides: bloom dynamics in a restricted subtropical lagoon under shifting climatic conditions. *Estuar. Coasts* 38, 886–904. doi: 10.1007/s12237-014-9874-6

Phlips, E. J., Badylak, S., Nelson, N. G., and Havens, K. E. (2020). Hurricanes, El Niño and harmful algal blooms in two sub-tropical Florida estuaries: direct and indirect impacts. *Sci. Rep.* 10:1910. doi: 10.1038/s41598-020-058771-4

Phlips, E. J., Badylak, S., Nelson, N. G., Hall, L. M., Jacoby, C. A., Lasi, M. A., et al. (2021). Cyclical patterns and a regime shift in the character of phytoplankton blooms in a restricted sub-tropical lagoon, Indian River Lagoon, Florida, USA. *Front. Mar. Sci.* doi: 10.3389/fmars.2021.730834

Romnée, A., Ervard, A., and Trachte, S. (2015). Methodology for a stormwater sensitive urban watershed design. *J. Hydrol.* 530, 87–102. doi: 10.1016/j.hydrol.2015.09.054

Rosario-Llantin, J., and Zarillo, G. A. (2021). Flushing rates and hydrodynamic characteristics of Mosquito Lagoon (Florida, USA). *Environ. Sci. Pollut. R.* 28, 30019–30034. doi: 10.1007/s11356-021-12367-1

Seitzinger, S. P., Mayorga, E., Bouwman, A. F., Kroeze, C., Beusen, A. H. W., Billen, G., et al. (2010). Global river nutrient export: a scenario analysis of past and future trends. *Glob. Biogeochem. Cycles* 24:GBOA08. doi: 10.1029/2009GB003587

Sigua, G. C., and Tweedale, W. A. (2003). Watershed scale assessment of nitrogen and phosphorus loadings in the Indian River Lagoon basin, Florida. *J. Environ. Manag.* 67, 363–372. doi: 10.1016/s0301-4797(02)00220-7

Smith, R. M., and Kaushal, S. S. (2015). Carbon cycle of an urban drainage basin: export, sources, and metabolism. *Biogeochemistry* 12, 279–294. doi: 10.1007/s10533-015-0151-y

St. Johns River Water Management District [SJRWMD] (2020b). *Data From: Environmental Data for Indian River Lagoon*. Palatka, FL: St. Johns River Water Management District.

St. Johns River Water Management District [SJRWMD] (2020a). *Data From: Continuous Water Quality Monitoring for Indian River Lagoon*. Palatka, FL: St. Johns River Water Management District.

Stallard, R. F. (1998). Terrestrial sedimentation and the carbon cycle: coupling weathering and erosion to carbon burial. *Glob. Biogeochem. Cycles* 12, 231–257. doi: 10.1029/98gb00741

Steward, J. S., Virnstein, R. W., Lasi, M. A., Morris, L. J., Miller, J. D., Hall, L. M., et al. (2006). The impacts of the 2004 hurricanes on hydrology, water quality, and seagrass in the Central Indian River Lagoon. Florida. *Estuar. Coasts* 29, 954–965. doi: 10.1007/BF02798656

Steward, J. S., Virnstein, R. W., Morris, L. J., and Lowe, E. F. (2005). Setting seagrass depth, coverage, and light targets for the Indian River Lagoon System, Florida. *Estuaries* 28, 923–935. doi: 10.1007/BF02696020

Tetra Tech Inc, and Closewaters LLC (2021). *Save Our Indian River Lagoon Project Plan Update 2021*. Melbourne, FL: Brevard County Natural Resources Management.

Trefry, J. H., Fox, A. L., Trocine, R. P., Fox, S. L., and Beckett, K. M. (2019). *Trends for Inputs of Muck Components From Rivers, Creeks and Outfalls to the Indian River Lagoon*. Melbourne, FL: Brevard County Natural Resources Management.

Trefry, J. H., and Trocine, R. P. (1991). "Collection and analysis of marine particles for trace elements," in *Marine Particles: Analysis and Characterization, Geophysical Monograph 63*, eds D. C. Hurd and D. W. Spencer (Washington, DC: American Geophysical Union), 311–315.

Trefry, J. H., and Trocine, R. P. (2011). Metals in sediments and clams from the Indian River Lagoon, Florida: 2006-7 versus 1992. *Florida Sci.* 74, 43–62.

Trenberth, K. E., and Asrar, G. R. (2014). Challenges and opportunities in water cycle research: WCRP contributions. *Surv. Geophys.* 35, 515–532. doi: 10.1007/s10712-012-9214-y

United States Department of Agriculture (2009). "Chapter 7 – Hydrologic soil groups," in *National Engineering Handbook: Part 630 – Hydrology*, (Washington, DC: United States Department of Agriculture). Available online at: https://directives.sc.egov.usda.gov/OpenNonWebContent.aspx?content=22526.wba

United States Geological Survey [USGS] (2020d). *USGS 02251000 South Prong St Sebastian River Near Sebastian, FL*. Reston, VA: United States Geological Survey.

United States Geological Survey [USGS] (2020b). *USGS 02249500 Crane Creek at Melbourne FL*. Reston, VA: United States Geological Survey.

United States Geological Survey [USGS] (2020c). *USGS 02250030 Turkey Creek at Palm Bay FL*. Reston, VA: United States Geological Survey.

United States Geological Survey [USGS] (2020a). *USGS 02249007 Eau Gallie River at Heather Glen Circle at Melbourne FL*. Reston, VA: United States Geological Survey.

Van Mooy, B. A. S., Krupke, A., Dyhrman, S. T., Fredricks, H. F., Frischkorn, K. R., Ossolinski, J. E., et al. (2015). Major role of planktonic phosphate reduction in the marine phosphorus redox cycle. *Science* 348, 783–785. doi: 10.1126/science.sss8181

Viers, J., Dupré, B., and Gaillardet, J. (2009). Chemical composition of suspended sediments in world rivers: new insights from a new data base. *Sci. Total Environ.* 407, 853–868. doi: 10.1016/j.scitotenv.2008.09.053

Wang, J., Yan, W., Chen, N., Li, X., and Lu, L. (2015). Modeled changes of DIN:DIP ratios in the Changjiang River in relation to Chl-α and DO concentrations in

adjacent estuary. *Estuar. Coastal Shelf Sci.* 166, 153–60. doi: 10.1016/j.ecss.2014.11.028

Watanabe, A., Tsutsuki, K., Inoue, Y., Maie, N., Melling, L., and Jaffé, R. (2014). Composition of dissolved organic nitrogen in rivers associated with wetlands. *Sci. Total Environ.* 493, 220–228. doi: 10.1016/j.scitotenv.2014.05.095

Wettstein, C. A., Noble, C. V., and Slaubaugh, J. D. (1987). *Soil Survey of Indian River County, Florida*. Washington, DC: United States Department of Agriculture, Soil Conservation Service.

Wetz, M. S., and Yoskowitz, D. W. (2013). An 'extreme' future for estuaries? Effects of extreme climatic events on estuarine water quality and ecology. *Mar. Pollut. Bull.* 69, 7–18. doi: 10.1016/j.marpolbul.2013.01.020

Wiegner, T. N., Seitzinger, S. P., Gilbert, P. M., and Bronk, D. A. (2006). Bioavailability of dissolved organic nitrogen and carbon from nine rivers in the eastern United States. *Aquat. Microb. Ecol.* 43, 277–287. doi: 10.3354/ame043277

Conflict of Interest: The authors declare that the research was conducted in the absence of any commercial or financial relationships that could be construed as a potential conflict of interest.

Publisher's Note: All claims expressed in this article are solely those of the authors and do not necessarily represent those of their affiliated organizations, or those of the publisher, the editors and the reviewers. Any product that may be evaluated in this article, or claim that may be made by its manufacturer, is not guaranteed or endorsed by the publisher.